


8-1-2016

Ionic Polymer-Metal Composite Actuators Based on Nafion Blends with Functional Polymers

Jungsoo Nam
University of Nevada, Las Vegas

Follow this and additional works at: <https://digitalscholarship.unlv.edu/thesesdissertations>

 Part of the [Chemistry Commons](#), and the [Mechanical Engineering Commons](#)

Repository Citation

Nam, Jungsoo, "Ionic Polymer-Metal Composite Actuators Based on Nafion Blends with Functional Polymers" (2016). *UNLV Theses, Dissertations, Professional Papers, and Capstones*. 2799.
<http://dx.doi.org/10.34917/9302956>

This Thesis is protected by copyright and/or related rights. It has been brought to you by Digital Scholarship@UNLV with permission from the rights-holder(s). You are free to use this Thesis in any way that is permitted by the copyright and related rights legislation that applies to your use. For other uses you need to obtain permission from the rights-holder(s) directly, unless additional rights are indicated by a Creative Commons license in the record and/or on the work itself.

This Thesis has been accepted for inclusion in UNLV Theses, Dissertations, Professional Papers, and Capstones by an authorized administrator of Digital Scholarship@UNLV. For more information, please contact digitalscholarship@unlv.edu.

IONIC POLYMER-METAL COMPOSITE ACTUATORS
BASED ON NAFION BLENDS WITH FUNCTIONAL POLYMERS

By

Jungsoo Nam

Bachelor of Chemistry and Nano Science
Ewha Womans University
2014

A thesis submitted in partial fulfillment
of the requirements for the

Master of Science - Chemistry

Department of Chemistry and Biochemistry
College of Science
The Graduate College

University of Nevada, Las Vegas
August 2016



Thesis Approval

The Graduate College
The University of Nevada, Las Vegas

June 21, 2016

This thesis prepared by

Jungsoo Nam

entitled

Ionic Polymer-Metal Composite Actuators Based on Nafion Blends with
Functional Polymers

is approved in partial fulfillment of the requirements for the degree of

Master of Science - Chemistry
Department of Chemistry and Biochemistry

Dong-Chan Lee, Ph.D.
Examination Committee Chair

Kathryn Hausbeck Korgan, Ph.D.
Graduate College Interim Dean

Gary Kleiger, Ph.D.
Examination Committee Member

Kathleen Robins, Ph.D.
Examination Committee Member

Kwang Kim, Ph.D.
Graduate College Faculty Representative

ABSTRACT

Ionic Polymer-Metal Composite Actuators based on Nafion Blends with Functional Polymers

by

Jungsoo Nam

Dr. Dong-Chan Lee, Exam Committee Chair

Associate Professor of Chemistry

University of Nevada, Las Vegas

Ionic polymer metal composites (IPMCs) have been an attractive research subject for use in underwater robotic applications, biomedical and biomimetic application owing to their great potential as actuators, artificial muscles, and more. IPMC is synthetic composite nanomaterial of ion exchange membranes and metal electrode. Although both components are important, the properties of ion exchange membranes should be emphasized since it is responsible of the path for the mobile ions to migrate when voltage is applied to exhibit deformation. Most of the researches that have been done on IPMCs used commercially available Nafion as their ion exchange membranes. However, its high cost, limitations in thermal and mechanical properties are some of the disadvantages that needs to be modified. In this thesis, we chose two different polymers, poly(vinyl alcohol-co-ethylene) [P(VA-co-E)] and polyimide [PI], as blending partners of Nafion in order to overcome these disadvantages while maintaining high ionic conductivity. In chapter 2, blend ion exchange membranes of Nafion and P(VA-co-E) were casted using physical blending method. The membranes were characterized by Fourier transform infrared spectroscopy and differential scanning calorimetry. IPMCs based on these membranes were fabricated by deposition of platinum electrode onto

their surface via electroless plating process. The electrode surface of prepared IPMCs was measured using two point probe method. The cross-sectional morphologies of the IPMCs were characterized through Scanning electron microscopy and Energy-dispersive X-ray spectroscopy analysis was done. The electromechanical performances (displacement and blocking force) of the prepared IPMC actuators were further characterized. In chapter 3, blend ion exchange membranes of Nafion and PI were obtained by casting of Nafion and poly(amic acid) [PAA]membranes and the following thermal imidization. Same characterizations were done as in chapter 3. The IPMC actuators with the blend Nafion membranes demonstrated comparable electromechanical performance to the Nafion membrane by either lowering the manufacturing cost or improving thermal and mechanical properties.

ACKNOWLEDGEMENTS

First of all, I would like to thank Professor Dong-Chan Lee deeply for guiding me with patience and giving me this great opportunity to learn here at University of Nevada, Las Vegas. Not only have I learned knowledge, but I have also been taught to solve problems that I confront throughout my life. I would like to express deep appreciation for Professor Kwang J Kim for giving me opportunity to learn new field, encouraging me to be a better person, and supporting me throughout the years. I would also like to show appreciation to my committee members, Professor Kathleen Robins and Professor Gary Kleiger for their precious time, support, encouragement, and suggestions.

I would like to thank Dr. Taeseon Hwang for being supportive at all times and teaching me a lot. Without his help, I would not have been able to finish my study. Thank you, Taeseon. I would also like to thank Dr. Viljar Palmre for helping me with characterizations. I also thank my group member, Kelly Zaugg, who was supportive throughout my school years, making my time at UNLV so great.

I am thankful to the faculty and staff members of Chemistry Department, especially Professor David Hatchett, Professor Jun Yong Kang, Professor Paul Forster, Carolyn Hatchett, Mark Miyamoto, and Debora Maters, for the opportunity to learn, giving me advice, and helping me.

Finally, I would like to express my deepest gratitude and love to my family for always being on my side and supporting me spiritually: My parents Jae-Do Nam and Kiesoon Ahn, my sister Jungah Nam, and my brother Junghoon Nam.

TABLE OF CONTENTS

ABSTRACT	iii
ACKNOWLEDGEMENTS	v
LIST OF TABLES	viii
LIST OF FIGURES	ix
LIST OF ABBREVIATIONS	xi
CHAPTER 1	1
1.1. Ionic Polymer - Metal Composites	1
1.2 Ion Exchange Membranes	3
1.3 Research objectives.....	6
CHAPTER 2.....	7
2.1 Introduction.....	7
2.2 Materials	8
2.3 Preparation of Membranes.....	9
2.4 Characterizations of membranes	10
2.4.1 Chemical Structures of prepared membranes.....	10
2.4.2 Thermal properties of prepared membranes.....	12
2.5 Fabrication of IPMCs	14
2.6 Characterizations of IPMCs.....	17
2.6.1 Cross-sectional morphologies and chemical compositions of IPMCs.....	17
2.6.2 Voltage, current, displacement responses, and bending strain of IPMCs.....	18
2.6.3 Blocking forces of IPMCs.....	22
2.7 Conclusions.....	24
CHAPTER 3.....	26
3.1 Introduction.....	26
3.2 Materials	28
3.3 Preparation of membranes	28
3.4 Characterizations of membranes.....	30

3.4.1	Chemical structures of prepared membranes	30
3.4.2	Thermal properties of prepared membranes.....	33
3.4.3	Mechanical properties of prepared membranes.....	34
3.5	Fabrication of IPMCs	36
3.6	Characterizations of IPMCs.....	38
3.6.1	Cross-sectional morphologies of IPMCs	38
3.6.2	Voltage, current, displacement responses, and bending strain of IPMCs.....	39
3.6.3	Blocking forces of IPMCs.....	43
3.7	Conclusions.....	44
3.8	Future studies.....	45
REFERENCES		47
CURRICULUM VITAE		55

LIST OF TABLES

Table 2.1	Composition, drying condition, and thickness of the membranes: Nafion, NPVAE-34, and NPVAE-55.....	9
Table 2.2	Glass transition temperature, melting transition temperature, and heat of fusion of P(VA- <i>co</i> -E), NPVAE-34, and NPVAE-55.....	13
Table 2.3	The electrode surface resistance of prepared IPMCs after electroless plating. (measured by two - point probe method).....	16
Table 3.1	Detailed composition of materials used in the prepared samples after casting....	30
Table 3.2	The electrode surface resistance of prepared IPMCs after electroless plating. (measured using two-point probe method).....	37

LIST OF FIGURES

Figure 1.1	Schematic actuation principle of IPMC.....	3
Figure 1.2	Chemical structure of Nafion in acid form.....	5
Figure 2.1	Photographic images of the prepared membranes: (a) Nafion, (b) NPVAE-34, and (c) NPVAE-55. (Size = 2.5 × 2.5 cm).....	10
Figure 2.2	The FT-IR spectra of (a) Nafion (N117), (b) cast Nafion, (c) P(VA-co-E), (d) NPVAE-34, and (e) NPVAE-55 membranes.....	11
Figure 2.3	DSC thermograms of Nafion, NPVAE-34, NPVAE-55, and P(VA-co-E). First heating scan at 10 °C/min.....	13
Figure 2.4	Photographs of the prepared IPMCs after platinum plating: (a) Nafion, (b) NPVAE - 34, and (c) NPVAE - 55. (Size=0.5 x 2.0 cm).....	16
Figure 2.5	The SEM images of cross-sectional morphologies [(a) Nafion, (b) NPVAE-34, and (c) NPVAE-55] and EDX results [(d) Nafion, (e) NPVAE-34, and (f) NPVAE-55] of the fabricated IPMCs. (g) Chemical composition of main elements in the membranes.....	18
Figure 2.6	The experimental setup to measure bending displacement of the IPMCs.....	19
Figure 2.7	Measured voltage, current, displacement responses, and bending strain at ±3 V AC square-wave under (a) 0.5 Hz and (b) 1 Hz of the IPMC actuators: Nafion, NPVAE-34, and NPVAE-55.	21
Figure 2.8	Photographs of the IPMC actuators, (a) Nafion, (b) NPVAE-34, and (c) NPVAE-55 with/without applying voltage (±3 V, AC) under frequencies of 0.1, 0.5, and 1.0 Hz.....	22
Figure 2.9	The experimental setup to measure blocking force of the IPMCs Hz.....	23
Figure 2.10	Measured blocking force responses in time at 3 V, DC for IPMC actuators: (a) Nafion, (b) NPVAE-34, and (c) NPVAE-55.....	24
Figure 3.1	Summary of preparing blend membrane of polyimide and Nafion.....	27
Figure 3.2	Photographs of prepared membranes after thermal imidization. (condition: 180 °C, 12 h, vacuum) (a) Nafion, (b) NPI-6, (c) NPI-12, and (d) NPI-18. (Size = 1.0 × 1.0 cm).....	30
Figure 3.3	FT-IR spectra of polyamic acid film (untreated) and polyimide film (treated)	

before and after thermal imidization (condition : 180 °C, 12 h, vacuum) for regions (a) 4000-700 cm^{-1} and (b) 2200-700 cm^{-1}31

Figure 3.4 FT-IR spectra of Nafion, NPI-6, NPI-12, NPI-18, and polyimide for regions (a) 4000-700 cm^{-1} and (b) 2100-700 cm^{-1}32

Figure 3.5 Thermogravimetric analysis (TGA) using the Q500 (TA) increasing temperature 30-700 °C, heating rate 10 °C/min in nitrogen environment: (a) TGA and (b) TGA derivative curve of the membranes.....34

Figure 3.6 DMA results of membranes Nafion 117 (■), NPI-6 (●), NPI-12 (▲), and PI (◆). The results are (a) storage modulus, (b) loss modulus, and (c) $\tan \delta$ with a frequency range from 0.01 to 20 Hz in tensile mode. The storage modulus (◀), loss modulus (▶), and $\tan \delta$ (★) of samples at 10 Hz are shown in (d).....36

Figure 3.7 Photographic images of the fabricated IPMCs: (a) Nafion 117 and (b) NPI-18..37

Figure 3.8 SEM images of prepared IPMCs : (a) Nafion, (b) NPI-6, (c) NPI-12, and (d) NPI-18.....39

Figure 3.9 The actuation performance of the IPMC actuators (Nafion 117, NPI-18): measured voltage, current, displacement responses, and bending strain at ± 3 V, AC square-wave under (a) 0.1 Hz, (b) 0.5 Hz, and (c) 1.0 Hz. Superimposed image of video captures of NPI-18 actuator at 0.1 Hz is also included in (a) clearly exhibiting the bounce-back effect of PI-incorporated actuator system.....41

Figure 3.10 Photographic images of prepared IPMC actuators, (a) Nafion 117, (b) NPI-18 with/without applying voltage (± 3 V, AC) under varied frequency (0.1, 0.5, and 1.0 Hz).....43

Figure 3.11 Blocking force responses in time at 3 V, DC for IPMC actuators comparing Nafion 117 and NPI-18.....44

LIST OF ABBREVIATIONS

IPMC	Ionic polymer – metal composite
EAP	Electroactive polymers
PSSA	Polystyrene sulfonic acid
SPEEK	Sulfonated poly(ether ether ketone)
PVDF	Polyvinylidene fluoride
EVOH	Ethylene-co-vinyl alcohol
P(VA-co-E)	Poly(vinyl alcohol-co-ethylene)
PAA	Poly(amic acid)
PI	Polyimide
FT-IR	Fourier transform infrared spectroscopy
DSC	Differential scanning calorimetry
TGA	Thermogravimetric Analysis
DMA	Dynamic mechanical analysis
SEM	Scanning electron microscope
EDX	Energy-dispersive X-ray spectroscopy

CHAPTER 1

INTRODUCTION

1.1. Ionic Polymer - Metal Composites

Ionic electroactive polymers (EAPs) are polymers that show change in size or shape when electrical stimulation is applied. These EAPs form composite with metal on the surface which is electrically conductive, undergoing large amount of bending deformation while sustaining large forces when electrically stimulated. There are many types of EAPs such as ionic polymer gel [1-4], dielectric elastomer [5, 6], carbon nanotube films [7, 8], ionic polymer-metal composites (IPMCs) [9-11], etc. Among these EAPs, IPMCs are the most promising field.

IPMCs are synthetic composite nanomaterials that exhibit deformation under an applied voltage or electric field. IPMCs are known for flexibility since they use polymers as base materials, low operating voltage (less than 5V), high strain rate, and the ability to operate in water [12, 13]. These properties make the IPMC an attractive research subject for use in underwater robotic applications [14, 15], fluid flow sensor applications [16], biomedical and biomimetic application such as artificial muscles [17-19], and more.

In 1949, Kuhn and Katchalsky reported that certain co-polymers may contract and expand chemically like a synthetic muscle [20, 21]. As an example, three dimensional networks which contain poly(acrylic acid) [PAA] are insoluble in water but swell extremely in water when base is added and contract extremely when acid is added [22]. After these studies, many researches have been conducted regarding chemically stimulated polymer deformation

including deformation of long cylindrical polymer gel [23], chemically stimulated pseudo-muscular actuation [24, 25], and more.

The first paper that was reported for electrochemical transduction of polyelectrolyte system such as PAA – poly(vinyl chloride) [PVC] was published in 1965 [26]. Later, Oguro et al. developed the first IPMC that was made of Nafion (N115) with platinum electrodes on both sides which shows electrochemical deformation when electrically stimulated [27].

IPMCs are composed of two parts, ionic polymer membrane and metal electrode. Ionic polymer membranes such as Nafion or Flemion are electrochemically plated on the surface of the membrane with metals such as gold or platinum. When an IPMC is fabricated, it contains cations, anions, and water molecules inside. When a small voltage is applied to it (generally less than 5V), hydrated mobile ions (either cations or anions) in the ion exchange membrane move toward anode or cathode, forming volumetric gradient or pressure gradient between electrodes on both sides. This gradient is responsible for the deformation of the IPMC.

In this thesis, we used Nafion as a base material for the ion exchange membrane. Since Nafion has sulfonate group that is negatively charged, these anions are fixed once they are fabricated into ion exchange membrane. Mobile ions are cations. When IPMC is immersed in water and electrically stimulated, cations in the ion exchange membrane get hydrated with water molecules and move toward the anode. This movement of hydrated cations results in pressure gradient between the electrodes leads to bending of the IPMC. Hydrated cations that moved toward the anode expands the anode side while contracting the cathode side, forming bending from the cathode to the anode direction [9]. When alternating current (AC) is applied, the anode and the cathode would alternately change, forming continuous bending of IPMC to two opposite directions. Movements of hydrated cations and water molecules inside the membrane of IPMC that creates the deformation are shown in Figure 1.1.

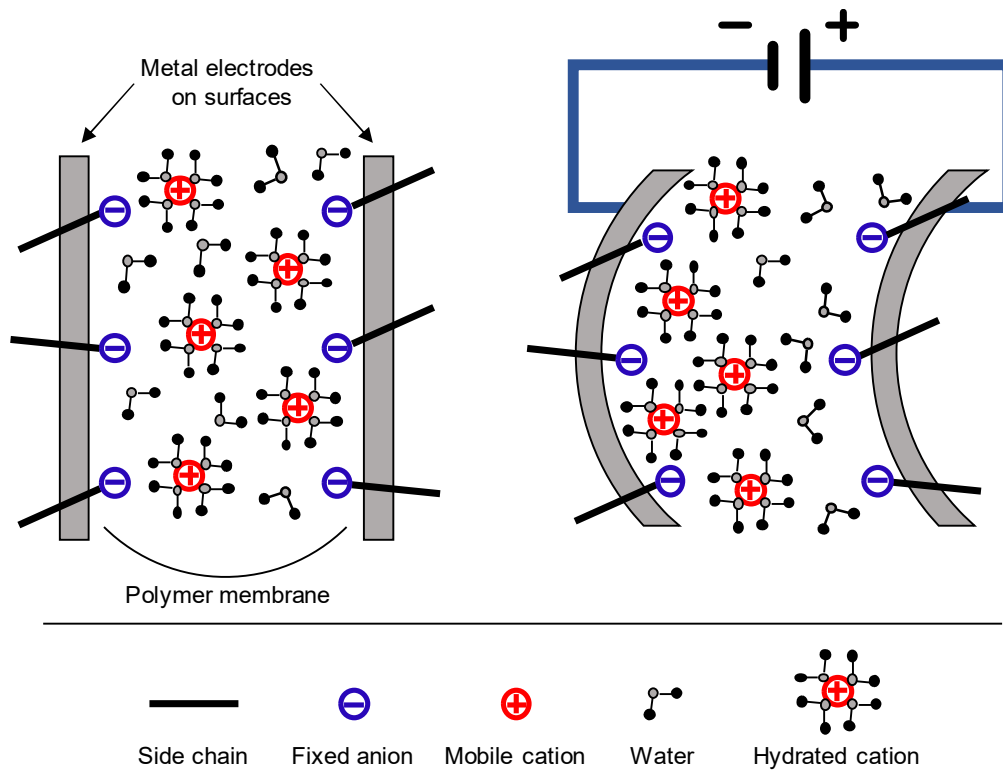


Figure 1.1 Schematic actuation principle of IPMC [9, 28].

1.2 Ion Exchange Membranes

Ion exchange membranes are fundamental materials to fabricate IPMCs and a very significant factor that largely influences the performance of IPMCs. The term ion exchange membrane refers to membrane that is designed to transport ions selectively across the polymeric membrane owing to ionic groups present in the membrane. Depending on the type of ionic groups attached, there are two types of ion exchange membranes; (1) cation exchange membrane and (2) anion exchange membrane. Cation exchange membranes contain fixed

anionic groups that allow the passage of cations and block anions. In reverse, anionic exchange membranes contain fixed cationic groups that allow the passage of anions and block cations.

Although Flemion can be used to fabricate IPMCs [29, 30], the most commonly used commercially available material for fabricating IPMCs is Nafion [31, 32], which was used for this thesis projects. Flemion and Nafion are both perfluorinated polymers, which differ in the functional groups. Flemion has carboxylate (R-COO^-) and Nafion has sulfonate (R-SO_3^-) as anionic functional groups. Research on Flemion-based actuators has been limited compared to that on Nafion because of the limitation of adequate computational tool to describe the electrochemical-mechanical response of Flemion-based IPMCs [33], low force (5 gf max) working in aqueous environment [34], and high stiffness compared to Nafion [35].

Nafion is known for its flexibility, light weight, immediate bending response, softness, low actuating voltage ($< 5 \text{ V}$), large bending deformation, commercial availability, appropriate mechanical robustness, good chemical stability, and high proton conductivity [36]. Nafion has high ion conductivity of around 0.1 S cm^{-1} in $1 \text{ M H}_2\text{SO}_4$ at $20 \text{ }^\circ\text{C}$ measured using a DC current pulse [37], which is important value to be a good ion exchange membrane.

Nafion consists of two parts, backbone and functional group as shown in Figure 1.2. The hydrophobic backbone gives mechanical strength to the ion exchange membrane and functional group which is sulfonate (SO_3^-) allows transportation of cations. The proton (H^+) attached to the sulfonate group as shown in Figure 1.2 can be replaced with other common mobile cations that are used in IPMC membranes such as lithium, sodium, and potassium. The functional group draws hydrated cations from side to side between two electrodes, producing bending movement.

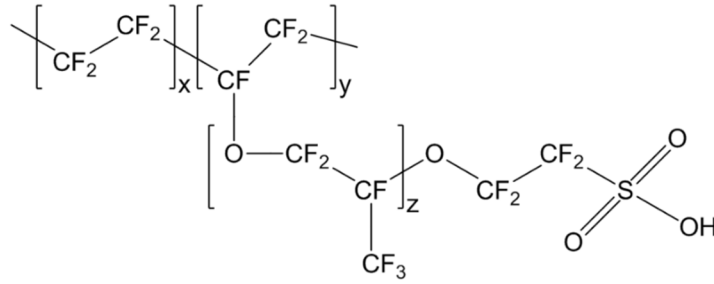


Figure 1.2 Chemical structure of Nafion in acid form [38].

When DC voltage is applied for long periods, Nafion-based actuators initially bend toward the anode, and undergo back relaxation by bending back toward the cathode. This is due to the leakage of water molecules to the anode side and it has been the major drawback of Nafion-based IPMCs, along with high cost and low blocking force [39]. There have been many studies to overcome the drawbacks by modifying the ion exchange membrane: Han et al. [40] fabricated new IPMC actuator using fluoropolymers grafted with polystyrene sulfonic acid [PSSA] as ion exchange membrane and investigated the actuation of the middle parts of the IPMCs and the blocking force under DC 2 V. They concluded that IPMCs based on the PSSA-grafted fluoropolymers can produce several times larger displacement than the Nafion-based IPMC with a similar thickness and successfully eliminated the back relaxation which was the major drawback of Nafion-based IPMCs. Jeon et al. [41] chose sulfonated poly(ether ether ketone) [SPEEK] and SPEEK/polyvinylidene fluoride [PVDF] as ion exchange membrane and tested the actuation performances. They reported that SPEEK/PVDF membrane-based IPMC showed larger actuation than that of SPEEK membrane-based IPMC under the applied DC voltages, harmonic sinusoidal voltages, and excitation frequencies. At 3 V DC, the blocking force of the SPEEK/PVDF-based IPMC actuator was higher than that of the SPEEK-based

IPMC actuator and lower than that of the Nafion-based actuator. They concluded that the good actuation performance of SPEEK/PVDF-based actuator might be due to the unique microstructure. Phillips and Moore [42] fabricated IPMC based on a sulfosuccinic acid-modified ethylene-co-vinyl alcohol [EVOH] membrane. The displacement and blocking force of the IPMC were lower than those compared to the Nafion-based IPMC. They concluded that this is due to the slow diffusion of water that passes through the disorganized ionomer morphology formed in the sulfonated EVOH matrix.

1.3 Research objectives

Despite the excellent electromechanical performances of Nafion, there are drawbacks which include high-cost and limitation in the property modification. To overcome the problems, we chose two different types of polymers, poly(vinyl alcohol-co-ethylene) [P(VA-co-E)] and polyimide [PI] as blend partners of Nafion. The main objective of this thesis is to fabricate IPMC actuators using blend ion exchange membranes of Nafion with P(VA-co-E) and PI that show comparable electromechanical properties to Nafion-only acuator while reducing the cost and improving thermal and mechanical properties.

This thesis presents simple but effective approaches to reduce the cost and improve the physical properties of Nafion-based IPMC via solution-based polymer blending. In Chapter 1, we chose P(VA-co-E) as the blending partner of Nafion to lower the manufacturing cost while maintaining the electromechanical properties. In Chapter 2, we chose PI as the blending partner of Nafion to modify thermal and mechanical properties of Nafion.

CHAPTER 2

IPMC BASED ON

NAFION / POLY(VINYL ALCOHOL-CO-ETHYLENE) BLENDS

2.1 Introduction

Poly(vinyl alcohol-co-ethylene) [P(VA-co-E)] is nontoxic and biocompatible polymer which has considerable chemical resistance [43], high mechanical strength, low fouling potential, and excellent film forming properties [44]. Since it could be compatible with Nafion owing to their similar structures that contain both hydrophobic and hydrophilic part, we chose P(VA-co-E) as a blending partner with Nafion to fabricate a blend ion exchange membrane.

As mentioned earlier, Nafion is the most generally used ion exchange membrane material used for the IPMC actuators, and this is due to its advantages which include good chemical stability, high proton conductivity, commercial availability, and appropriate mechanical robustness [45-47]. Although Nafion – based IPMC actuators show good actuation performances under low voltage stimulus, high cost of Nafion is the major drawback for its practical applications [47]. Therefore, there have been many attempts to replace Nafion and develop other materials that are lower in cost for ion exchange membranes used in IPMC actuators [37, 45, 48]. In attempt, fluorinated acrylic copolymer membrane, non-fluorinated hydrocarbon polymers, and sulfonated polymers have been investigated [49-51]. Some of the research was focused on developing composites of Nafion with different kinds of fillers such as montmorillonite, titanium dioxide, and silica [52-54]. These attempts of replacing Nafion, however, have been only partly successful. Hence, it is important to continue seeking for

polymers that can replace Nafion for the use in IPMC actuators.

The objective of the work is to prepare homogeneous Nafion/polymer composite membranes through solution casting method which is physical blending method, and to study the electromechanical properties of the membrane and compare it with Nafion. We chose P(VA-co-E) as the blending polymer, since it is considered as a polymer matrix that can be used to make new cost-saving ionomers owing to its ability to form film, high modulus, high strength, and hydrophilicity [55-57].

After investigating different conditions to cast high quality blend membranes, the chemical structure of the blend membranes was characterized by FT-IR and thermal properties were characterized by DSC. We fabricated IPMCs from the blend membranes and characterized the cross-sectional morphologies by SEM. Also, the chemical composition was characterized by EDX. The electromechanical performances including displacement testing and blocking forces were also tested.

2.2 Materials

Nafion dispersion (5 wt.%) was purchased from DuPont™. P(VA-co-E) and dimethyl sulfoxide (DMSO) were purchased from Sigma-Aldrich to use for the preparation of the blend membranes. Ammonium hydroxide (NH_4OH), tetraammineplatinum (II) chloride hydrate ($\text{Pt}(\text{NH}_3)_4\text{Cl}_2 \cdot x\text{H}_2\text{O}$), and sodium borohydride (NaBH_4) were purchased from Sigma-Aldrich to use for platinum plating. Hydrazine monohydrate ($\text{H}_2\text{NNH}_2 \cdot \text{H}_2\text{O}$) and hydroxylamine hydrochloride ($\text{H}_2\text{NOH} \cdot \text{HCl}$) were purchased from Sigma-Aldrich to use as the reducing agents. Lithium chloride (LiCl) was purchased from Sigma-Aldrich to use for ion exchange

process.

2.3 Preparation of Membranes

The cast membrane of Nafion was prepared by solution casting of 10 mL of Nafion dispersion in a Teflon mold (Size = $2.5 \times 2.5 \times 0.5$ cm) at 30 °C overnight. Blend membranes, NPVAE-34 and NPVAE-55 were prepared by solution casting of 10 mL of mixed Nafion solution with P(VA-co-E) / DMSO (5 wt.%) solution in the Teflon mold at 60 °C overnight. The detailed composition of materials after drying is summarized in Table 2.1.

Table 2.1 Composition, drying condition, and thickness of the membranes: Nafion, NPVAE-34, and NPVAE-55

Samples	Weight ratio of P(VA-co-E) : Nafion	Drying condition	Thickness (μm)
Nafion	0 : 100	30 °C, overnight	280
NPVAE-34	34 : 66	60 °C, overnight	290
NPVAE-55	55 : 45	60 °C, overnight	350

Photographic images of prepared samples of Nafion, NPVAE-34, and NPVAE-55 membranes are shown in Figures 2.1. Nafion – only membrane was transparent but as P(VA-co-E) blended into Nafion, the blend membranes became opaque and the stiffness of the

membranes increased as the content of P(VA-co-E) increased. The prepared NPVAE-34 and NPVAE-55 membranes are cost effective up to 30 and 50 % respectively, compared to pure Nafion (based on the current prices of the chemicals as of 2016).

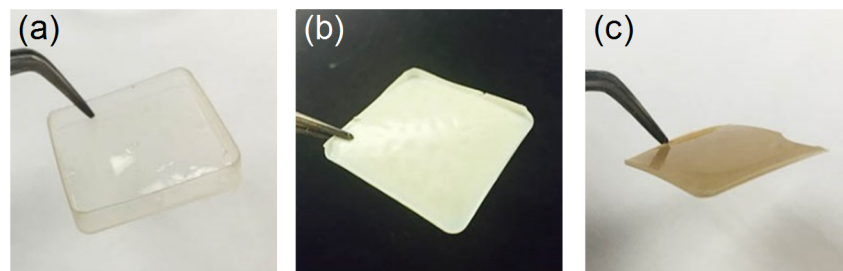


Figure 2.1 Photographic images of the prepared membranes:

(a) Nafion, (b) NPVAE-34, and (c) NPVAE-55 (Size = 2.5 × 2.5 cm).

2.4 Characterizations of membranes

2.4.1 Chemical Structures of prepared membranes

The blend membranes were characterized with FT-IR spectroscopy to confirm the presence of both constituents, Nafion and P(VA-co-E) in the membranes. The results are shown in Figure 2.2. FT-IR spectra of NPVAE-34 and NPVAE-55 are shown in Figures 2.2 (d) and (e), respectively. Spectra of (a) Nafion 117, (b) cast Nafion, and (c) P(VA-co-E) membranes were also included as reference.

The FT-IR spectra of Figures 2.2 (a) commercially available Nafion 117 membrane and (b) cast Nafion membrane were very similar, showing peaks at 1153 cm^{-1} (CF_2 stretching,

asymmetric) and 1213 cm^{-1} (CF_2 stretching, symmetric) which are characteristic to Nafion [58]. These peaks are shown in the spectra of NPVAE-34 and NPVAE-55, confirming the presence of Nafion in the blend membranes. For the spectrum of P(VA-co-E), a broad peak at $3200\text{-}3400\text{ cm}^{-1}$ (O-H stretching), peaks at 2924 cm^{-1} (C-H stretching, aliphatic), and 1443 cm^{-1} (C-H bending, aliphatic) which are characteristic to P(VA-co-E). These peaks are shown in the spectra of NPVAE-34 and NPVAE-55, confirming the presence of P(VA-co-E) in the blend membranes. The FT-IR results clearly confirms the presence of both components, Nafion and P(VA-co-E) in the blend membranes.

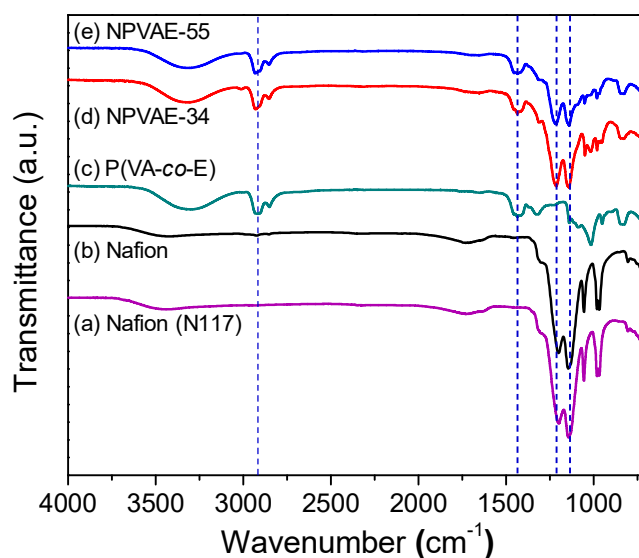


Figure 2.2 The FT-IR spectra of (a) Nafion (N117), (b) cast Nafion, (c) P(VA-co-E), (d) NPVAE-34, and (e) NPVAE-55 membranes.

2.4.2 Thermal properties of prepared membranes

Thermal properties of the blend membranes were characterized by DSC as shown in Figure 2.3 and the resulting glass transition temperature (T_g), melting transition temperature (T_m), and heat of fusion (ΔH_f) are shown in Table 2.2. While P(VA-co-E) showed T_g at 43 °C and T_m at 165 °C, Nafion did not show distinguishable transition. As the content of Nafion increases, T_g significantly decreases from 58.9 °C (P(VA-co-E)) to 45.4 °C (NPVAE-55) to 42.6 °C (NPVAE-34). For T_m , while P(VA-co-E) and NPVAE-55 shows similar values, 165.2 °C and 165.5 °C, respectively, NPVAE-34 shows a decreased value of 161.1 °C. The heat of fusion, ΔH_f , decreases constantly as the content of Nafion increases from 45.7 J/g ((P(VA-co-E))) to 25.5 J/g (NPVAE-55) to 15.2 J/g (NPVAE-34). Decreasing trend in T_g , T_m , and ΔH_f as increasing of the content of Nafion indicates the reducing crystallinity of P(VA-co-E) owing to the blending of the amorphous Nafion. The DSC results indicate that P(VA-co-E) and Nafion be a miscible blend system.

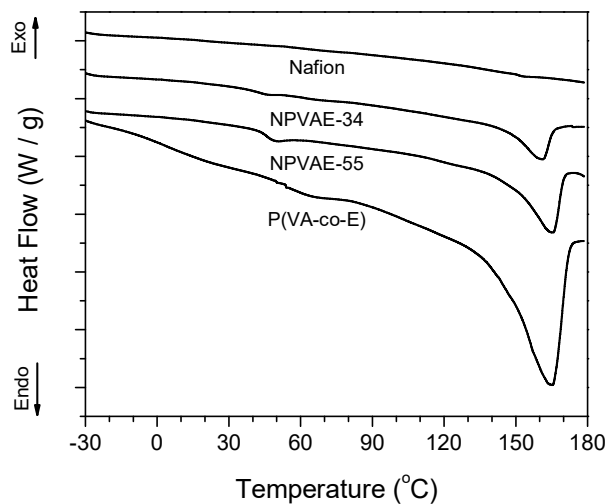


Figure 2.3 DSC thermograms of Nafion, NPVAE-34, NPVAE-55, and P(VA-*co*-E). [First heating scan at 10 °C/min under nitrogen.]

Table 2.2 Glass transition temperature, melting transition temperature, and heat of fusion of P(VA-*co*-E), NPVAE-34, and NPVAE-55

Samples	T_g (°C)	T_m (°C)	ΔH_f (J/g)
P(VA- <i>co</i> -E)	58.9	165.2	45.7
NPVAE-55	45.4	165.5	25.5
NPVAE-34	42.6	161.1	15.2

2.5 Fabrication of IPMCs

The membranes were sanded with sandpaper (800 / 1000 counts) in order to deposit more platinum particles onto the inner surface by increasing the surface area. It also helps increase the contact area of polymer and electrode. Sanding needs to be done in the direction perpendicular to the bending direction of the IPMC. After sanding, all membranes were cleaned to remove impurities before progressing to the primary plating process. Membranes were cleaned in 3 wt.% H_2O_2 solution at 70 °C for 40 minutes, 1 M H_2SO_4 aqueous solution at 60 °C for 40 minutes, D.I. water at 70 °C for 40 minutes, 1 M H_2SO_4 aqueous solution at 60 °C for 40 minutes, followed by cleaning in D.I. water at 40 °C for 40 minutes.

The next step, primary plating is an impregnation-reduction process on the roughened inner surface of the membranes. Membranes were soaked in 0.02M Pt (II) salt solution (tetraammineplatinum (II) chloride hydrate, $\text{Pt}(\text{NH}_3)_4\text{Cl}_2 \cdot x\text{H}_2\text{O}$) for 3.5 h and rinsed with D.I. water several times. To metalize the surface of the membranes, they were immersed in 350 mL aqueous solution containing NH_4OH (0.3 mL) and NaBH_4 (0.2g) at 60 °C for 2 h. 0.2g of NaBH_4 was added every 0.5 h. Membranes were cleaned in 1 M H_2SO_4 aqueous solution at 60 °C for 40 minutes, D.I. water at 70 °C for 40 minutes, 1 M H_2SO_4 aqueous solution at 60 °C for 40 minutes, followed by cleaning in D.I. water at 40 °C for 40 minutes. The primary plating procedure was repeated three times.

The secondary plating was processed to develop platinum on the outer surface of the membrane, on top of the inner platinum layer, to reduce the surface resistance of the electrode. The membranes were soaked in 350 mL of aqueous solution containing Pt (II) salt (0.2 g) and two reducing agents, 20 wt.% $\text{H}_2\text{NNH}_2 \cdot \text{H}_2\text{O}$ solution (1 mL) and 5 wt.% $\text{H}_2\text{NOH} \cdot \text{HCl}$ solution (2 mL) at 50 °C for 1 h and then 60 °C for 3 h. The reducing agents were added every 30 minutes for 4 h. Then, the composites were cleaned in 1 M H_2SO_4 aqueous solution at 60 °C

for 40 minutes, D.I. water at 70 °C for 40 minutes, 1 M H₂SO₄ aqueous solution at 60 °C for 40 minutes, followed by cleaning in D.I. water at 40 °C for 40 minutes. If the resistance is greater than 10-15 Ω, the entire procedure should be done up to two times. After all the process was done, the membranes were placed in 1 M LiCl solution overnight in order to replace protons with lithium ions. The platinum layers were successfully plated on to the surfaces of the membranes without cracks. The photographs of the fabricated IPMCs fabricated from Nafion, NPVAE-34, and NPVAE-55 membranes after electroless plating are shown in Figure 2.4.

The IPMCs were cut into rectangular shapes [0.5 × 2.0 cm] for further characterizations. The electrode surface resistance for the IPMCs was measured using two-point probe method and the results after each step of electroless plating is shown in Table 2.3. When the content of P(VA-co-E) increases in the blend membranes, the electrode resistance also increases. This may be due to the less impregnation of platinum complex ions into the membrane during electroless plating process. As an assumption, impregnation of platinum complex ions become harder as the content of P(VA-co-E) in the blend membranes increases. All values were less than 2.0 Ω/cm after secondary electroless plating which are appropriate compared to the previous work [46].



Figure 2.4 Photographs of the prepared IPMCs after platinum plating:
 (a) Nafion, (b) NPVAE-34, and (c) NPVAE-55 (Size=0.5 x 2.0 cm).

Table 2.3 The electrode surface resistance of prepared IPMCs after electroless plating
 (measured by two-point probe method).

Samples	1 st Primary plating (Ω/cm)	2 nd Primary plating (Ω/cm)	3 rd Primary plating (Ω/cm)	Secondary plating (Ω/cm)
Nafion	5.1 - 5.3	2.0 - 2.2	1.0 - 1.1	0.7 - 1.0
NPVAE-34	8.7 - 9.0	3.3 - 3.7	2.2 - 2.4	1.2 - 1.4
NPVAE-55	19.5 - 20.0	10.1 - 11.0	9.9 - 10.2	1.5 - 1.8

2.6 Characterizations of IPMCs

2.6.1 Cross-sectional morphologies and chemical compositions of IPMCs

The cross-sectional morphologies of fabricated IPMCs characterized by SEM and the according EDX results are shown in Figure 2.5. From the cross-sectional morphologies and the deposited layer of platinum on the surface of the membrane as shown in Figures 2.5 (a)-(c), it is observable that the thickness of platinum electrode layer decreases as the content of P(VA-co-E) in the membrane increases. The thickness of the platinum electrode decreases from 17 μm (Nafion) to 14 μm (NPVAE-34) to 10 μm (NPVAE-55). As mentioned earlier, as an assumption, impregnation of platinum complex ions become harder as the content of P(VA-co-E) in the blend membranes increases, resulting in thinner electrodes. EDX analysis of the cross-sectional SEM images are shown in Figures 2.5 (d)-(f). These results show the chemical composition of the fabricated IPMCs. Also, a graph that compares the number of counts of the elements C, O, and F in the Nafion and blend membranes is shown in Figure 2.5 (g). As the content of P(VA-co-E) in the membranes increases, the counts of C and O in the membranes increase while that of F decreases.

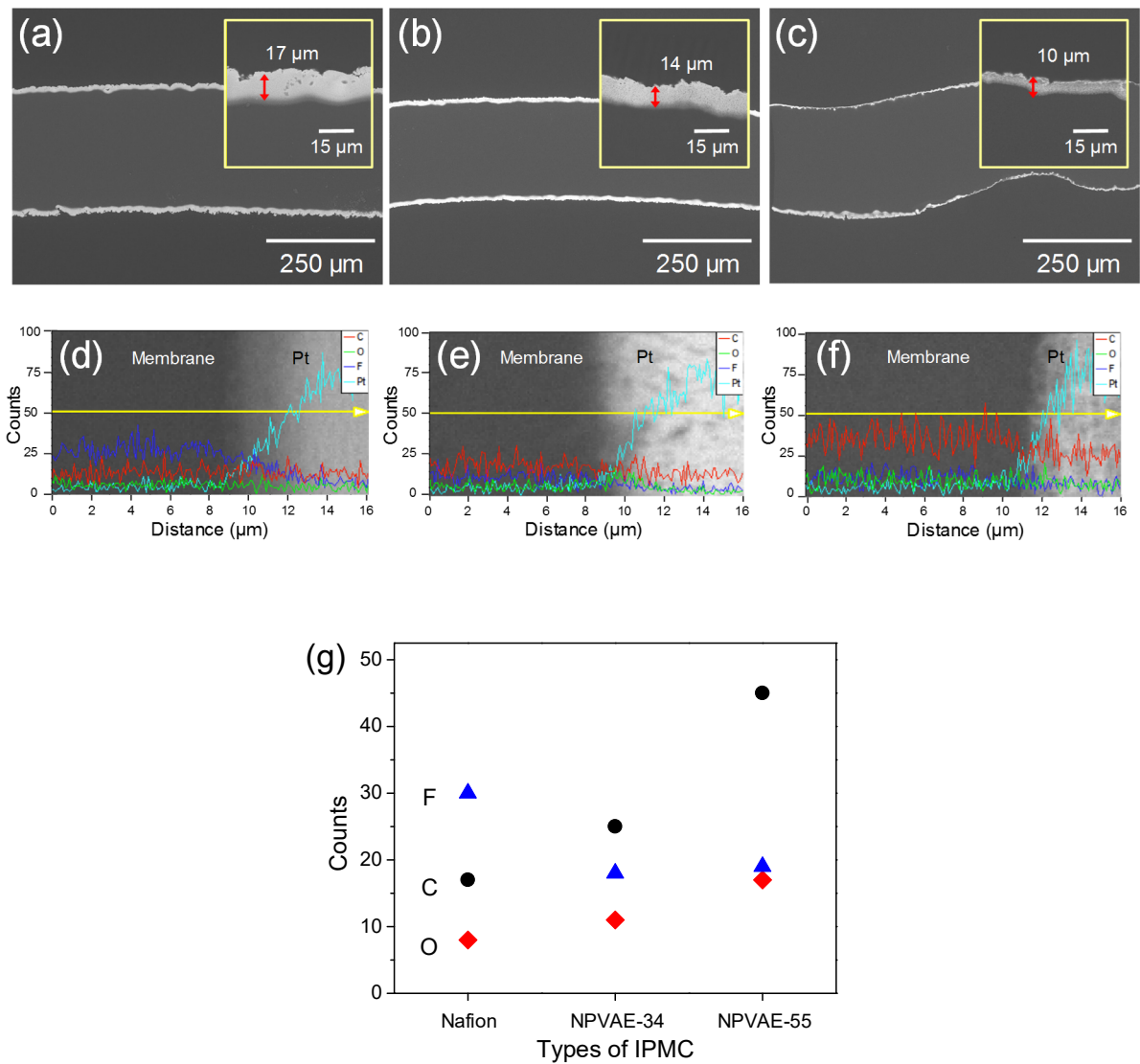


Figure 2.5 The SEM images of cross-sectional morphologies [(a) Nafion, (b) NPVAE-34, and (c) NPVAE-55] and EDX results [(d) Nafion, (e) NPVAE-34, and (f) NPVAE-55] of the fabricated IPMCs. (g) Chemical composition of main elements in the membranes.

2.6.2 Voltage, current, displacement responses, and bending strain of IPMCs

The actuation test is performed to observe the deflection at the tip of the IPMCs. The

deflection at the tip was measured by placing a laser 2mm ca. above the bottom edge of the IPMC where it gives the maximum displacement. Frequency analyzer was connected to the power source and the voltage was adjusted. The experimental setup is shown in Figure 2.6.

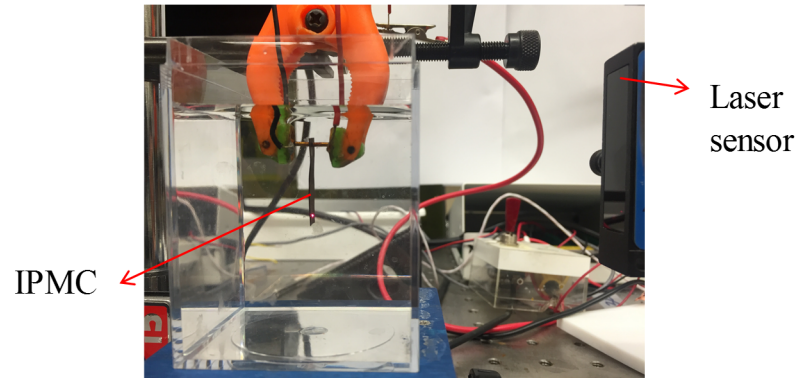


Figure 2.6 The experimental setup to measure bending displacement of the IPMCs.

Measured voltage, current, corresponding displacement responses, and bending strain of Nafion, NPVAE-34, and NPVAE-55 – based IPMCs at $\pm 3V$ AC (square wave input) at frequencies 0.5 and 1.0 Hz are shown in Figure 2.7. The bending strain (ϵ) was converted from displacement (δ) using the relation of $\epsilon \cong \frac{\delta t}{L^2 + \delta^2}$, where t is the thickness of the IPMC and L is the free length.

Among the three IPMC actuators, the Nafion – based IPMC actuator shows the highest displacement performance. NPVAE-55 shows the lowest electromechanical performance owing to the high electrode surface resistance and relatively high stiffness of the membrane.

Interestingly, NPVAE-34 – based IPMC actuator showed almost the similar displacement (2.5 mm) and bending strain (0.27 %) to that of the Nafion-only IPMC which showed displacement of 2.8 mm and bending strain of 0.26 %, under a low actuation frequency of 0.5Hz. However, under higher frequency of 1Hz, Nafion actuator shows displacement of 2.8 mm and bending strain of 0.29 % while NPVAE-34 actuator shows lower displacement (2.0 mm) and lower bending strain (0.21 %). Comparing 0.5Hz and 1 Hz, under higher frequency of 1Hz, the displacement and bending strain decreases for NPVAE-34 actuator due to the limited charging time [15].

Although NPVAE-34 IPMC actuator did not show higher actuation performance compared to Nafion actuator, it is important to focus on the fact that it shows a comparable electromechanical performance even though the content of Nafion is significantly reduced by 34 wt.% (weight percent ratio of Nafion:P(VA-co-E) = 66:34).

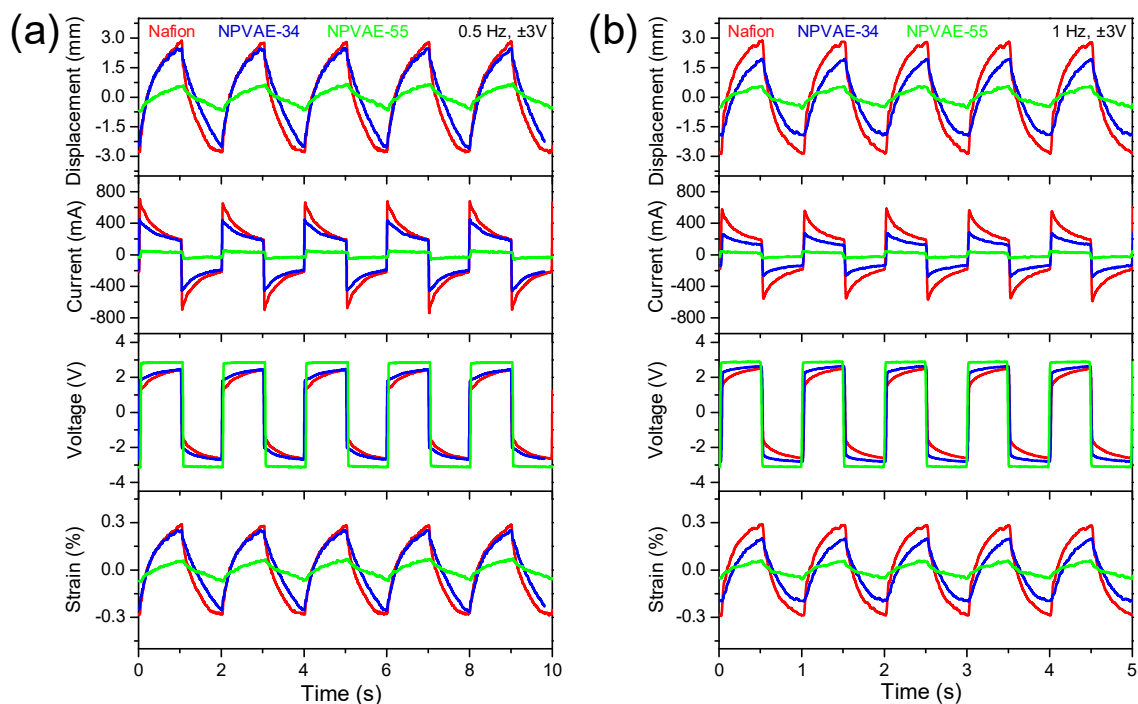


Figure 2.7 Measured voltage, current, displacement responses, and bending strain at ± 3 V AC square-wave under (a) 0.5 Hz and (b) 1 Hz of the IPMC actuators: Nafion, NPVAE-34, and NPVAE-55.

The photographs of the IPMC actuators at maximum displacement with/without applying voltage (± 3 V, AC) under frequency of 0.1, 0.5, and 1.0 Hz are shown in Figure 2.8. From Figures 2.8 (a) and (b), it is shown that the NPVAE-34 actuator show similar range of displacement as Nafion actuator. As the frequency decrease, from 1 to 0.5 to 0.1Hz, a clear difference in displacement response between the samples is observed. It is shown in Figure 2.8 (c) that NPVAE-55 actuator shows the lowest displacement due to the higher electrode surface resistance and higher stiffness compared to other samples. Again, the displacement of NPVAE-

34 actuator is comparable to that of Nafion actuator.

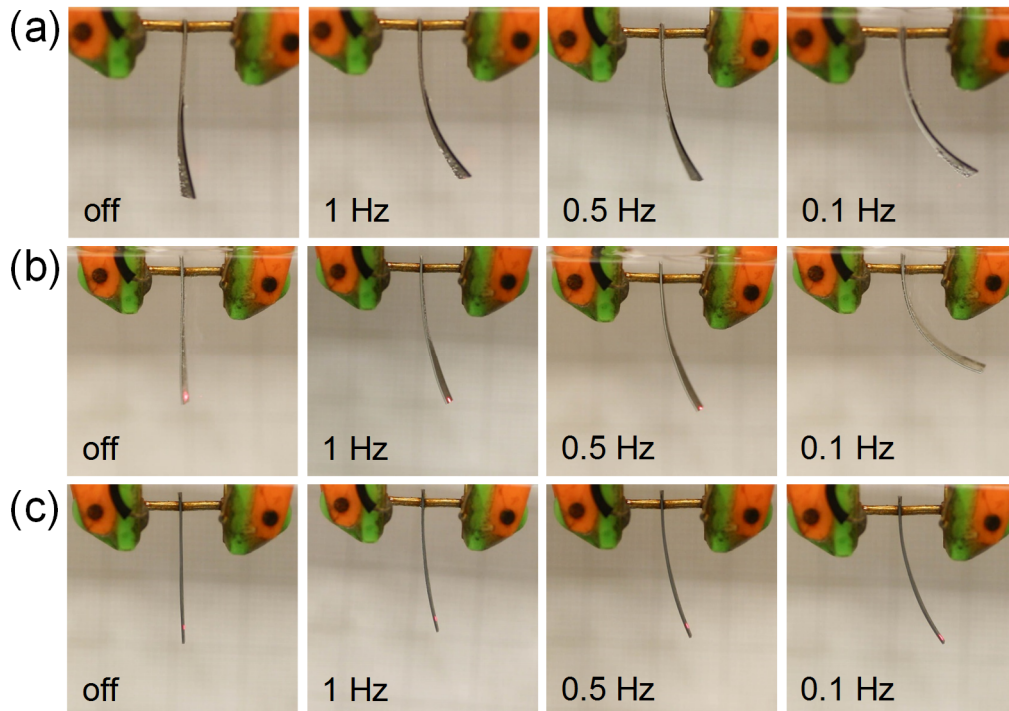


Figure 2.8 Photographs of the IPMC actuators, (a) Nafion, (b) NPVAE-34, and (c) NPVAE-55 with/without applying voltage (± 3 V, AC) under frequencies of 0.1, 0.5, and 1.0 Hz.

2.6.3 Blocking forces of IPMCs

The blocking force, which represents the electromechanical force formed at tip of IPMC at zero displacement, was measured under driving voltage of 3V, DC. The experimental setup is shown in Figure 2.9. Figure 2.10 shows the typical blocking force responses measured in time for Nafion, NPVAE-34, and NPVAE-55 actuators. The Nafion actuator show the highest

blocking force (13.5 mN) and the fastest response time (4.39 s) among three actuators. The measured highest blocking force of NPVAE-34 and NPVAE-55 is 12.3 mN at 4.54 s and 11.59 mN at 13.57 s, respectively. The results indicate that when the content of P(VA-co-E) in the membrane increases, the blocking force and response time of the actuators decreases, due to the increasing stiffness of the membrane. These results are correspondent with the displacement measurements that were discussed earlier.

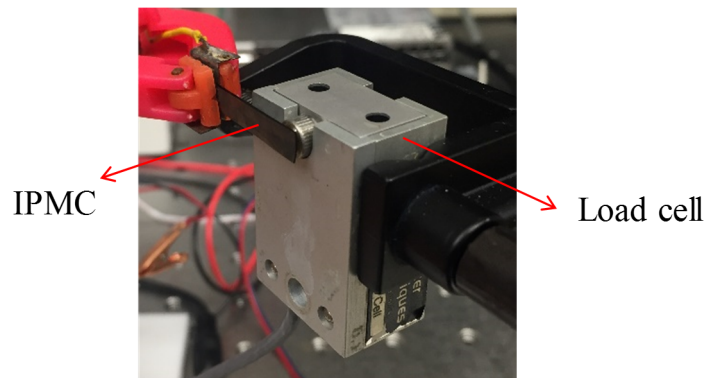


Figure 2.9 The experimental setup to measure blocking force of the IPMCs.

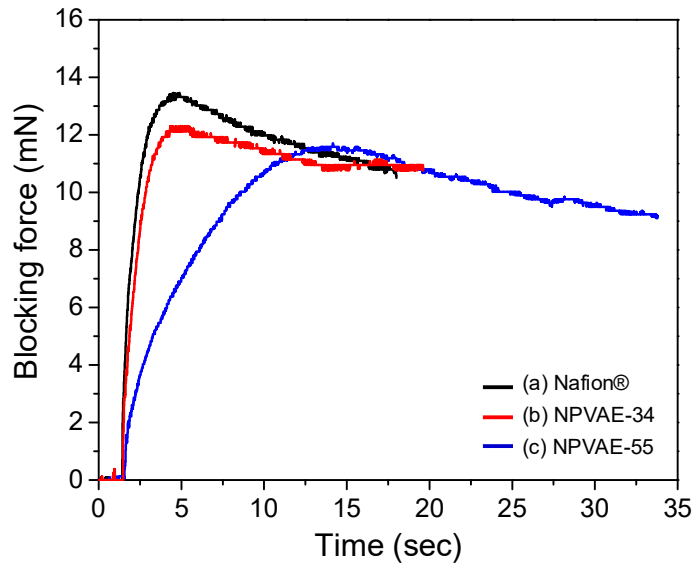


Figure 2.10 Measured blocking force responses in time at 3 V, DC for IPMC actuators: (a) Nafion, (b) NPVAE-34, and (c) NPVAE-55.

2.7 Conclusions

We successfully casted blend membranes of Nafion and P(VA-co-E), which were used to fabricate into IPMCs. The membranes were casted using solution casting method and were successfully blended. The blend membranes were characterized by FT-IR and DSC. FT-IR results confirmed the presence of both components, Nafion and P(VA-co-E) in the blend membranes and DSC results suggested the miscibility between the components. The blend membranes were fabricated into IPMCs using the conventional platinum electroless plating process of Nafion. The cross-sectional morphologies of the IPMCs and the chemical composition were characterized through SEM and EDX. Actuation performance of the actuators were also tested. As a result, NPVAE-34 showed comparable actuation performance

to that of Nafion even though we significantly reduced the content of Nafion by 34 wt.%. The work done in this chapter may give rise to modifying and improving the properties of Nafion using a simple and reproducible blending process, which can provide us with more cost-saving IPMC materials.

CHAPTER 3

IPMC BASED ON NAFION / POLYIMIDE BLENDS

3.1 Introduction

Aromatic PIs, is a class of high-performance polymers. Owing to their outstanding thermal and dimensional stability that have been widely studied for past years. Aromatic PIs are most widely used as coatings for microelectronic devices and high-temperature materials for the aerospace industry [59]. Because PI membrane, Kapton, is commercially available from DuPont and the outstanding thermal and mechanical properties are known, it was considered as a strong candidate for blending partner of Nafion. By blending PI with Nafion for making ion exchange membrane, the anticipated enhancements in features are specifically thermal properties [60], dimensional stability [61], and mechanical properties. There have been some reports on developing high-performance fuel cell applications [62-67] with sulfonated PI polyelectrolytes. Only limited examples are available for the electromechanical applications of sulfonated PIs [68, 69]. These examples utilize the lengthy chemical synthesis for sulfonated PI. There have been no prior example of employing physical blending of PI and Nafion. Therefore, we thought it would be promising if we could blend PI with Nafion successfully and use the blend membrane as an ion exchange membrane to fabricate IPMCs. Such blends could render better properties to Nafion which is potentially useful for the space utilization. The initial work was to find the optimum conditions to cast the blend membranes to obtain quality membranes and once they were obtained, we investigated the electromechanical

properties of the blend membranes.

Because of the rigidity of their chain and strong interchain interactions, most PIs (especially Kapton in Figure 3.1) are insoluble in organic solvents and intractable in their imide forms. Therefore, to make a blend ion exchange membrane of PI and Nafion, blend membrane of poly(amic acid) [PAA] precursor of PI and Nafion should be made first. This is due to the fact that PAA is soluble in organic solvent such as N-methyl-2-pyrrolidone [NMP] while PI is not. If PAA/Nafion membranes can be prepared, then PAA can be transformed to PI thermally, resulting in blend membranes of PI and Nafion. The scheme of the process is shown in Figure 3.1.

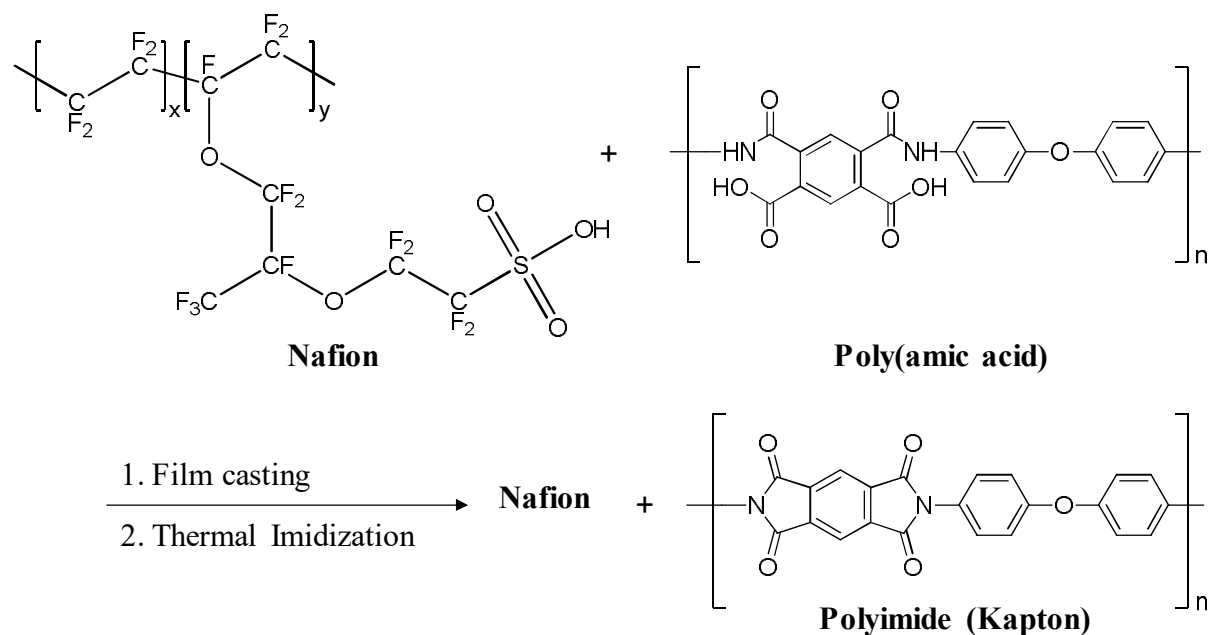


Figure 3.1 Summary of preparing blend membrane of PI and Nafion.

3.2 Materials

Poly(pyromellitic dianhydride-co-4,4'-oxydianiline), amic acid solution (11 wt.% \pm 5 wt.% in NMP/aromatic hydrocarbons (80 % / 20 % solvent ratio)) was purchased from Sigma-Aldrich. Alcohol-based Nafion dispersion (5 wt.%) and NMP were purchased from DuPontTM and TCI, respectively and were used for preparation of the blend membranes. Tetraammineplatinum (II) chloride hydrate ($\text{Pt}(\text{NH}_3)_4\text{Cl}_2 \cdot x\text{H}_2\text{O}$), ammonium hydroxide (NH_4OH), and sodium borohydride (NaBH_4) were purchased from Sigma-Aldrich and used for platinum plating. Hydrazine monohydrate ($\text{H}_2\text{NNH}_2 \cdot \text{H}_2\text{O}$) and hydroxylamine hydrochloride ($\text{H}_2\text{NOH} \cdot \text{HCl}$) were purchased from Sigma-Aldrich and used as the reducing agents. Lithium chloride (LiCl) was purchased from Sigma-Aldrich. Deionized (DI) water was used to clean the membrane and to prepare IPMCs.

3.3 Preparation of membranes

The membrane of Nafion was provided by solution casting of 30 mL of Nafion dispersion (5 wt.%, d: 0.87 g/mL) in a polystyrene mold ($r = 3.0$ cm, 1.9 depth) at 50 °C overnight. PI membrane was provided by solution casting of 12 mL of poly(pyromellitic dianhydride-co-4,4'-oxydianiline), amic acid solution (11 wt.% \pm 5 wt.% in NMP/aromatic hydrocarbons (80 % / 20 % solvent ratio), d : 1.066 g/mL) in aluminum foil mold ($r = 2.3$ cm, 1.27 cm depth) at 85 °C overnight.

Blend membranes of Nafion and PAA were prepared by solution casting of 21 mL of mixed Nafion solution (5 wt.%) with PAA / NMP solution (1.26 wt.%) through the following procedures. At first, 11 wt.% PAA solution (5.33 g, 5 mL) and NMP (41.36 g, 40 mL) were

added in a 100-mL beaker and stirred at room temperature for 1 hour. This 1.26 wt.% PAA solution (amount of PAA solution used for samples, NPI-6: 3.7 mL, 0.044 g, NPI-12: 6.6 mL, 0.086 g, NPI-18: 8.8 mL, 0.115 g, and NPI-30: 4.3 mL, 3.9 g) was mixed with 5 wt.% Nafion (amount of Nafion solution used for samples, NPI-6: 17.3 mL, 15.05 g, NPI-12: 14.4 mL, 12.53 g, NPI-18: 12.2 mL, 10.61 g, and NPI-30: 10.5 mL, 9.1 g) and the mixtures were stirred at 70 °C for NPI-6 (due to small amount of NMP) and room temperature for NPI-12, NPI-18, and NPI-30 for 1 hour. NPI-6, NPI-12, and NPI-18 were stirred at 60 °C overnight to evaporate solvent in a 50 mL beaker covered with Kimwipes®. In the case of NPI-30, temperature was set to 50°C since less solvent needed to be evaporated. The solutions were cooled to room temperature. None of the solutions precipitated, so each solution was poured into an aluminum foil mold (r = 2.3 cm, 1.27 cm in depth). The mold was placed in a desiccator connected to house vacuum and bubbles are removed for 10-20 minutes before casting. For samples NPI-6, NPI-12, and NPI-18, the mold was placed on a hot plate and was heated at 85 °C overnight. For NPI-30, the mold was placed in an oven at 70 °C for 2 days, since the same condition as other blends produced very brittle film. The cast membranes were taken out of the molds and placed in vacuum oven at 180 °C for 12 hours for thermal imidization to obtain Nafion/PI blend membranes. The photographs of prepared membranes are shown in Figure 3.2 and the detailed composition of materials is summarized in Table 3.1.

As shown in Table 3.1, NPI-6, NPI-12, NPI-18, and NPI-30 were named based on the weight ratio of PI to Nafion after drying solvents. The total amount of PI and Nafion in unit area respectively were calculated in mg/cm² and the weight ratio of the two components.

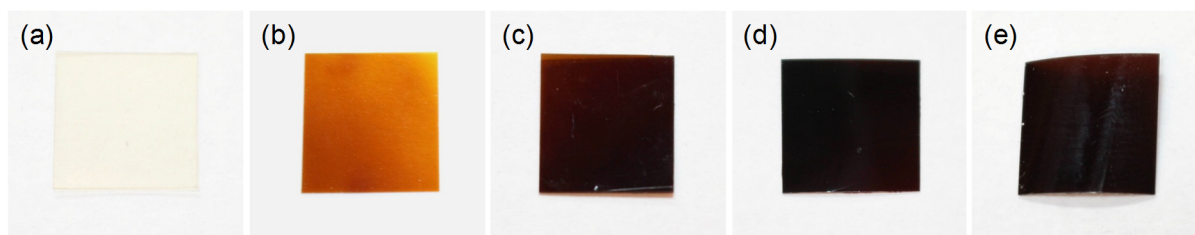


Figure 3.2 Photographs of prepared membranes after thermal imidization. (condition: 180 °C, 12 h, vacuum) (a) Nafion, (b) NPI-6, (c) NPI-12, (d) NPI-18, and (e) NPI-30 (Size = 1.0 × 1.0 cm).

Table 3.1 Detailed composition of materials used in the prepared samples after casting.

Sample name	Wt% ratio (PI : Nafion)	Total amount of PI (mg/cm ²)	Total amount of Nafion (mg/cm ²)	Casting condition	Thickness (μm)
Nafion	0 : 100	-	46.3	50°C, 5hrs	340
NPI-6	6 : 94	3.01	45.2	85°C, overnight	278
NPI-12	12 : 88	5.42	38		285
NPI-18	18 : 82	7.22	31.9		290
NPI-30	30 : 70	11.7	27.4	70°C, 2 days	310
PI	100 : 0	38.6	-	85°C, overnight	350

3.4 Characterizations of membranes

3.4.1 Chemical structures of prepared membranes

The samples were characterized by Fourier Transform Infrared Spectroscopy (FT-IR) after the imidization at 180 °C for 12 h in vacuum to confirm that they were successfully

imidized and both PI and Nafion components are in the blend membranes. Figure 3.3 shows spectra of PAA membrane and PI membrane before and after thermal imidization, which were compared as reference. Untreated PAA membrane showed peaks at 1714 cm^{-1} (C=O stretching, carboxylic), 1657 cm^{-1} (C=O stretching, amide), and 1540 cm^{-1} (N-H bending) [70]. After thermal imidization, 1714 cm^{-1} (C=O stretching, carboxylic) and 1657 cm^{-1} (C=O stretching, amide) were replaced with 1774 cm^{-1} (C=O stretching, asymmetric) and 1712 cm^{-1} (C=O stretching, symmetric) which are characteristic to PI. Moreover, other peaks at 1453 cm^{-1} (C=C stretching), 1367 cm^{-1} (C-N stretching, imide), and 1163 cm^{-1} (imide ring deformation) appeared, which indicated the successful thermal imidization [70].

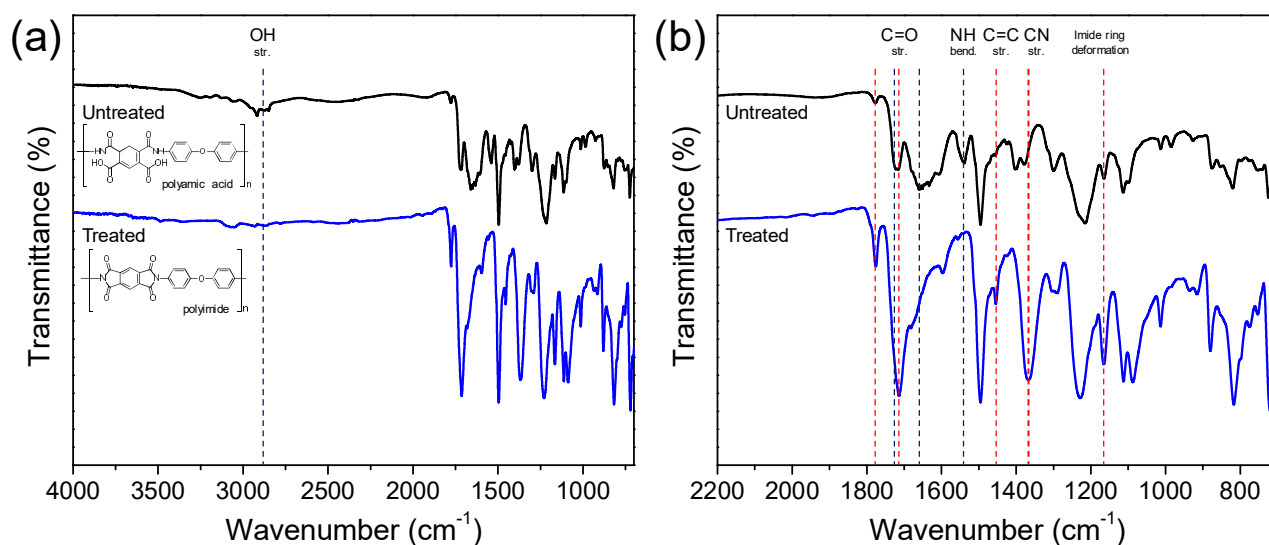


Figure 3.3 FT-IR spectra of PAA film (untreated) and PI film (treated) before and after thermal imidization (condition : $180\text{ }^{\circ}\text{C}$, 12 h, vacuum) for regions (a) $4000\text{-}700\text{ cm}^{-1}$ and (b) $2200\text{-}700\text{ cm}^{-1}$.

As shown in Figure 3.4, the blend membranes NPI-6, NPI-12, NPI-18, and NPI-30 showed peaks at 1780 cm^{-1} (C=O stretching, asymmetric), 1730 cm^{-1} (C=O stretching, symmetric), 1502 cm^{-1} (C=C stretching), and 1383 cm^{-1} (C-N stretching, imide). These peaks are characteristic to PI, confirming that the thermal imidization was successful and that PI is present in the blend membranes. Also, peaks at 1205 cm^{-1} (C-F stretching, asymmetric) and 1144 cm^{-1} (C-F stretching, symmetric) which are characteristic to Nafion were shown in NPI-6, NPI-12, NPI-18, and NPI-30, confirming the presence of Nafion in the blend membranes. [71] From FT-IR results, we confirmed the success of thermal imidization as well as incorporation of both polymers, PI and Nafion, in the blend membranes.

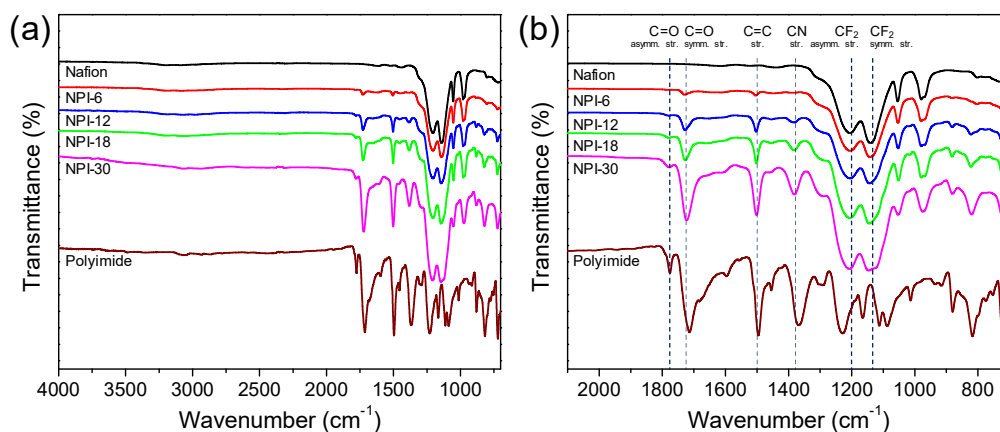


Figure 3.4 FT-IR spectra of Nafion, NPI-6, NPI-12, NPI-18, NPI-30 and PI for regions (a) $4000\text{-}700\text{ cm}^{-1}$ and (b) $2100\text{-}700\text{ cm}^{-1}$. All the spectra were normalized to have same intensity at 1207 cm^{-1} .

3.4.2 Thermal properties of prepared membranes

Thermal properties were characterized by TGA. The characterization was done at room temperature under nitrogen atmosphere, heating rate of 10 °C/min. As shown in Figure 3.5, PI membrane is stable at temperatures up to 550 °C. It shows a distinguishable thermal degradation around 550 - 600 °C. Also, the TGA derivative curve shows a broad transition peak at 315 °C and a sharp transition peak at 572 °C, with a total weight loss of 38 % after decomposition. Nafion membrane shows major weight loss stages around 325-380 °C and 420-570 °C. The TGA derivative curve shows two sharp transition peaks at 360 and 462 °C, with a total weight loss of 92% after decomposition.

Blend membranes NPI-6, NPI-12, NPI-18, and NPI-30 show two major weight loss stages around 325-380, 380-420, and a small third decomposition around 420-570 °C. The third decomposition increases as the content of PI increases. Differences in transition points compared to Nafion are not observable for TGA curve. In addition to sharp transition peaks at 360 and 462 °C, which are characteristic to Nafion, TGA derivative curve of blend membranes show broad transition peak at 315 °C and decomposition of PI as a shoulder at 565 °C. The total weight loss is 81 % for NPI-6 and NPI-12, and 77 % for NPI-18 and NPI-30. The TGA and TGA derivative curve of blend samples confirms the presence of both components, Nafion and PI, in the blends.

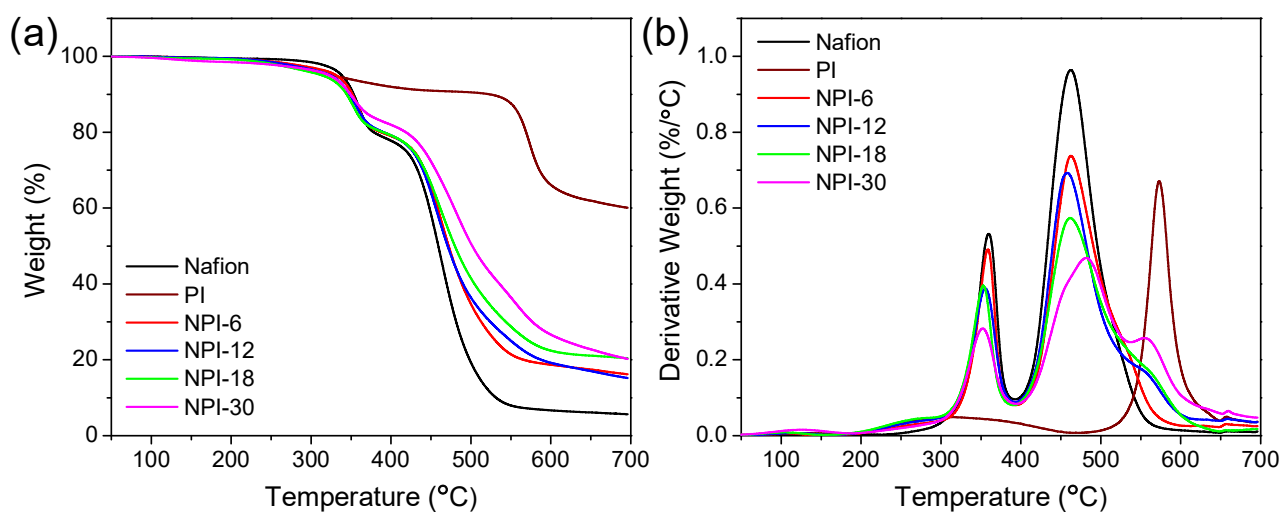


Figure 3.5 TGA using the Q500 (TA) increasing temperature 30-700 °C, heating rate 10 °C/min in nitrogen environment: (a) TGA and (b) TGA derivative curve of the membranes.

3.4.3 Mechanical properties of prepared membranes

A dynamic mechanical analysis using the Pyris Diamond DMA was conducted on Nafion 117, NPI-6, NPI-12, and PI membranes. DMA was not measured on NPI-18 and NPI-30 due to the stiffness of the membranes. DMA is important to understand the viscoelastic properties of the materials. The samples were cut into 0.5 cm × 2.5 cm. DMA was setup in tension, and they were oscillated at different frequencies (0.01, 0.02, 0.05, 0.1, 0.2, 0.5, 1, 2, 5, 10, 20 Hz). Measured storage modulus, loss modulus, and tangent delta are shown in Figure 3.6 (a)-(c), respectively. To clearly show the increasing and decreasing trends, storage modulus, loss modulus, and $\tan \delta$ of samples at 10 Hz are shown in Figure 3.6 (d). At 10 Hz, as the

content of PI in the membrane increased, the storage modulus (E') increased from 0.1563 (Nafion) to 0.5723 (NPI-6) to 1.619 (NPI-12) to 2.430 GPa (PI) (Figure 3.6a). In the case of loss modulus (E''), there was only minor changes: 0.0432 (Nafion), 0.1252 (NPI-6), 0.2343 (NPI-12), and 0.1366 GPa (PI) (Figure 3.6b). Therefore, damping properties ($\tan \delta = E''/E'$) [72-74] decreased from 0.2799 (Nafion) to 0.2191 (NPI-6) to 0.1448 (NPI-12) to 0.0562 (PI) as the content of PI increased (Figure 3.6c). The trends in E' , E'' , and $\tan \delta$ as a function of PI content were clearly shown in Figure 3.6d. We can conclude that by increasing the content of PI, we can increase the storage modulus, which represents the elastic property of the material. Meanwhile, loss modulus, which represents the viscous property, was not affected significantly up to 12% of PI, which result in the decrease in damping property. Although limited, selective tuning in the mechanical properties can be achieved by this simple physical blending. It should be noted that the DMA analysis of the blends with higher PI contents was not conducted due the brittleness of the samples.

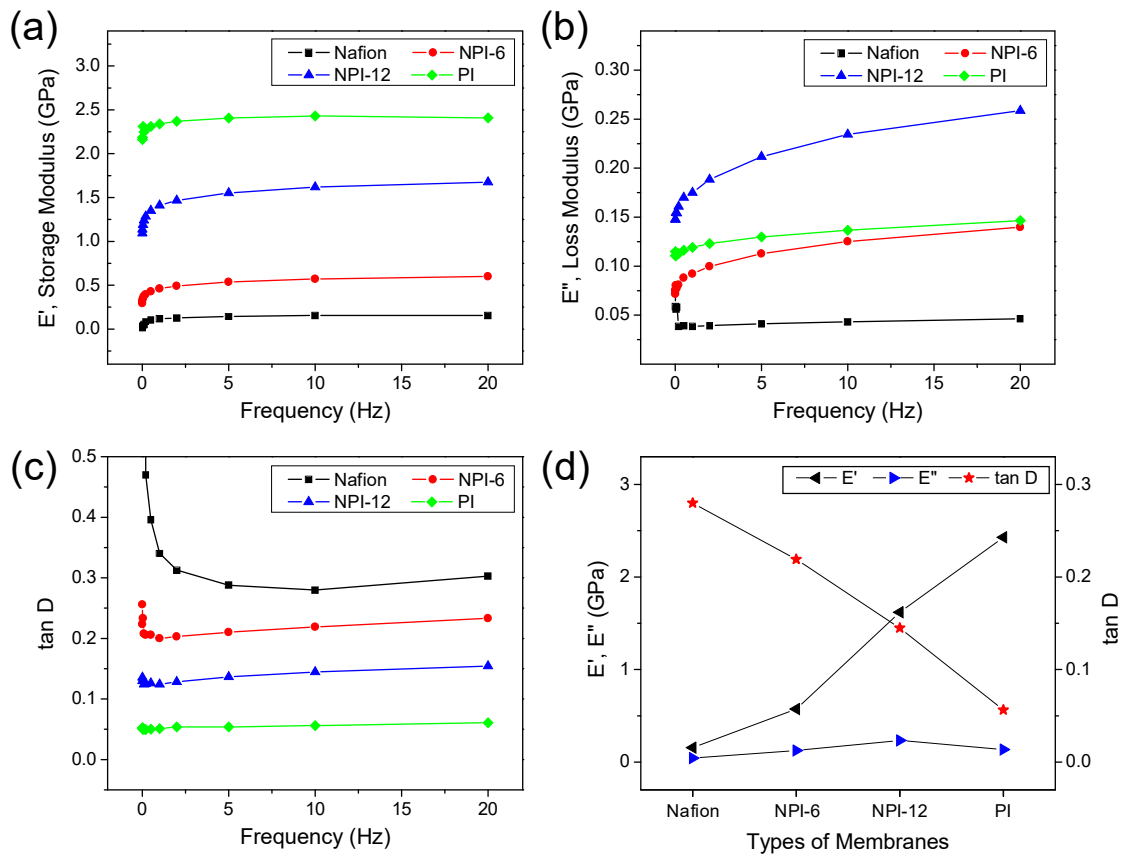


Figure 3.6 DMA results of membranes Nafion 117 (■), NPI-6 (●), NPI-12 (▲), and PI (◆). The results are (a) storage modulus, (b) loss modulus, and (c) $\tan \delta$ with a frequency range from 0.01 to 20 Hz in tensile mode. The storage modulus (◄), loss modulus (►), and $\tan \delta$ (★) of samples at 10 Hz are shown in (d).

3.5 Fabrication of IPMCs

The fabrication process followed the same procedures described in Chapter 2.5. The obtained IPMCs were cut into 0.5×2.5 cm rectangular shapes for further characterizations.

The measured electrode surface resistance of the prepared IPMCs after each plating step is summarized in Table 3.2. As mentioned earlier, solution casted Nafion, NPI-6, and NPI-12 show relatively high surface resistance that ranges 5.6-20.2 Ω/cm while NPI-18, NPI-30, and Nafion 117 show values less than 2 Ω/cm which are reasonable values compared to our previous work [47]. The photographic images of NPI-18, NPI-30, and Nafion 117 IPMCs are shown in Figure 3.7.

Table 3.2 The electrode surface resistance of prepared IPMCs after electroless plating (measured using two-point probe method).

	1 st primary plating (Ω/cm)	2 nd primary plating (Ω/cm)	3 rd primary plating (Ω/cm)	Secondary plating (Ω/cm)
Nafion (solution casted)	33.8 – 45.7	21.0 – 28.0	14.1 – 18.8	11.1 – 20.2
NPI-6	11.1 – 14.2	10.8 – 13.3	8.1 – 9.2	4.7 – 7.7
NPI-12	13.2 – 15.1	11.1 – 12.9	8.8 – 9.4	5.6 – 8.2
NPI-18	3.3 – 5.1	2.2 – 2.5	1.6 – 1.9	1.1 – 1.5
NPI-30	3.3 – 5.2	2.2 – 2.6	1.5 – 1.8	0.9 – 1.6
Nafion 117	4.2 – 5.3	2.8 – 3.1	1.6 – 1.9	1.3 – 1.7

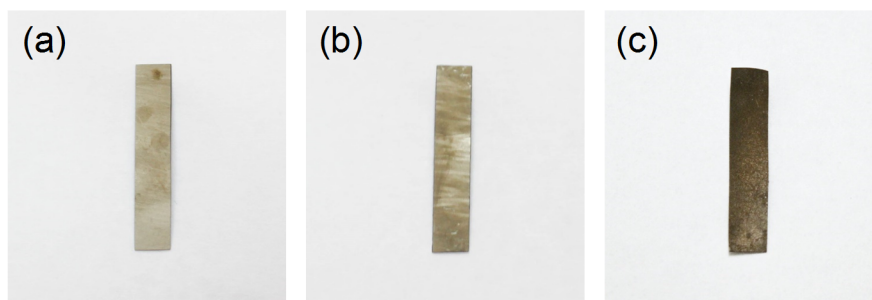


Figure 3.7 Photographic images of the fabricated IPMCs: (a) Nafion 117, (b) NPI-18, and (c) NPI-30.

3.6 Characterizations of IPMCs

3.6.1 Cross-sectional morphologies of IPMCs

The cross-sectional morphologies of solution casted Nafion, NPI-6, NPI-12, and NPI-18 – based IPMC actuators were characterized with SEM images as shown in Figure 3.8. For solution casted Nafion platinum complex ions were impregnated too deep into the polymer membrane during electroless plating process. For NPI-6, the thickness of the electrode was too thin (ca. 6 μm) and for NPI-12 membranes, platinum complex ions were impregnated too deep. As a result, solution casted Nafion, NPI-6, and NPI-12 – based IPMC showed high surface resistance of the electrode as shown in Table 3.2. Since the casting temperature was high for solution casted Nafion compared to previous work [47], fast evaporation of solvent may be responsible for uneven surface and high surface resistance of the Nafion-only IPMC. From the fact that NPI-18 shows good membrane quality and plating while NPI-6 and NPI-12 does not show good quality enough to make IPMCs, it can be concluded that the current casting condition is good for blend membranes that contain certain amount of PI. For the blend membranes with low PI content (up to 12 wt%), the casting casting temperature may need to be lowered to avoid fast evaporation.

Among the fabricated IPMCs, only NPI-18 and NPI-30 resulted in surface resistance (1.1-1.5 Ω/cm) less than 2.0 Ω/cm after secondary electroless plating, which is appropriate value compared to our previous work. Since the surface resistance of solution casted Nafion – based IPMC was too high, we prepared Nafion117 – based IPMC that resulted in surface resistance (1.3-1.7 Ω/cm) less than 2.0 Ω/cm to compare actuation performance of Nafion 117 and NPI-18 – based IPMCs.

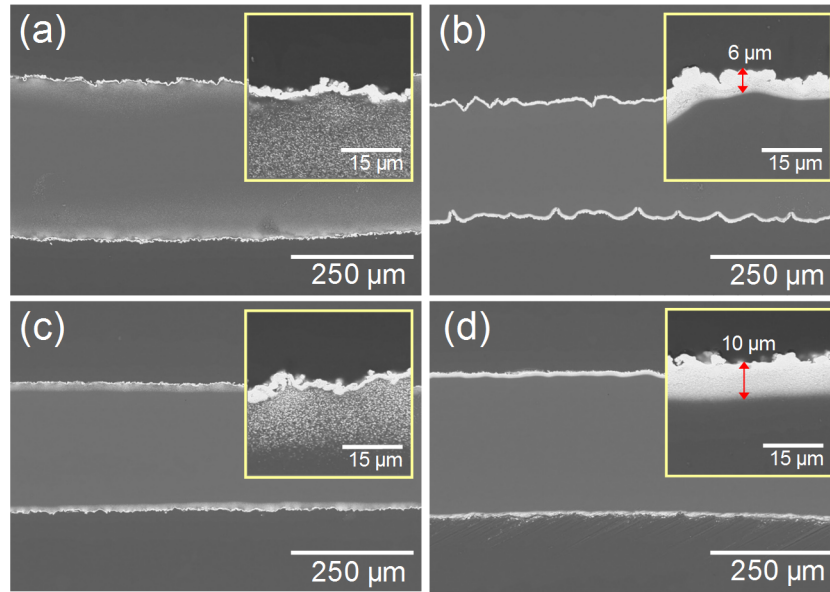


Figure 3.8 SEM images of prepared IPMCs : (a) Nafion (solution casted), (b) NPI-6, (c) NPI-12, and (d) NPI-18.

3.6.2 Voltage, current, displacement responses, and bending strain of IPMCs

Displacement responses of Nafion 117, NPI-18, NPI-30 IPMC actuators were measured at 0.1, 0.5, and 1 Hz. A displacement laser sensor kept track of the displacement at the tip while the voltage at the clamp was sensed by the circuit. Measured voltage, current, corresponding displacement responses, and bending strain of Nafion 117 and NPI-18 – based IPMC at $\pm 3V$ AC (square wave input) at frequencies 0.1, 0.5, and 1 Hz are shown in Figure 3.9. The bending strain (ϵ) was converted from displacement (δ) using the relation of $\epsilon \cong \frac{\delta t}{L^2 + \delta^2}$, where t is the thickness of the IPMC and L is the free length.

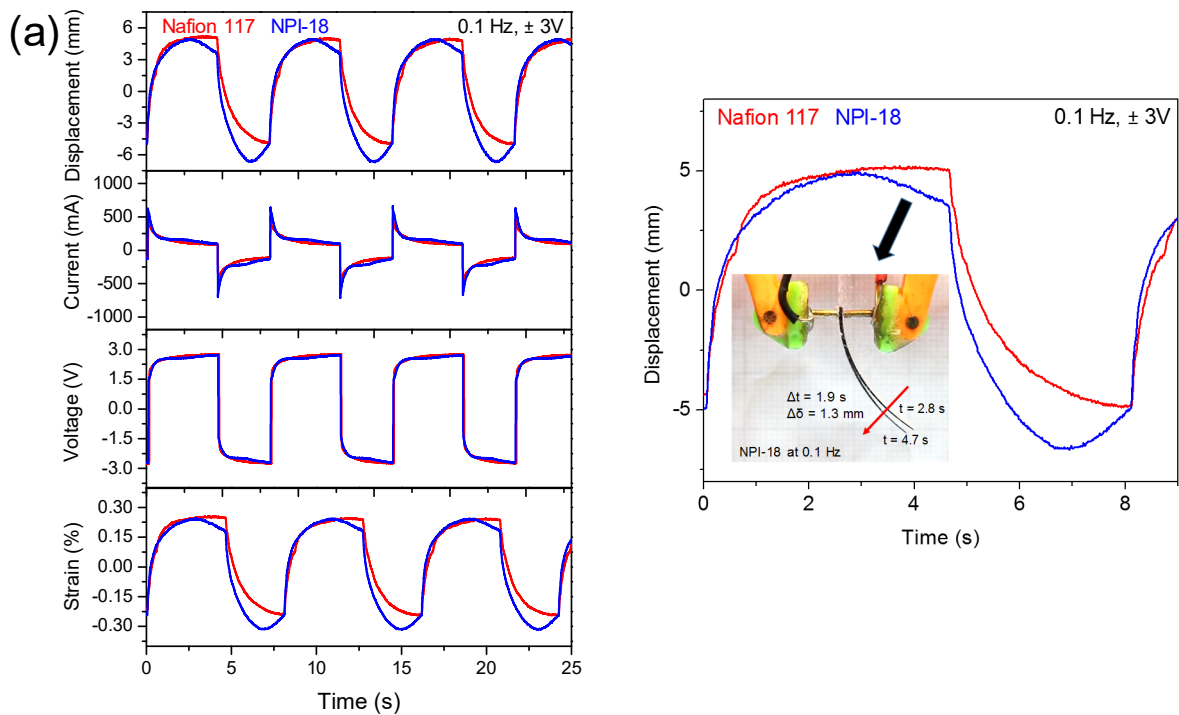
As shown in Figure 3.9 (a), the displacements of Nafion 117 and NPI-18 actuators at

0.1 Hz were 5.3 and 5.9 mm, and strains were 0.21 and 0.28 %, respectively. Superimposed image of video captures of NPI-18 actuator at 0.1 Hz is also included. The actuators show similar displacement performances up to 2.8 s. While NPI-18 shows a bounce-back effect, which does not maintain the maximum displacement but bounces back before bending to the opposite direction, from 2.8 to 4.7 s where displacement changes by 1.3 mm, which is not the case with the pristine Nafion 117. This result is in accordance with the DMA analysis. The increased elasticity may be responsible for the bounce-back effect. In the case of NPI-30, due to the experimental error, number of cycles of 0.1 Hz were not the same as Nafion 117 and NPI-18. However, important data from the displacement results was that the displacement was found to be 1.6 mm which was lower than Nafion 117 and NPI-18. This is due the stiffness of the blend.

At 0.5 Hz, as shown in Figure 3.9 (b), the displacement of Nafion 117 and NPI-18 actuators were almost same (3.8 mm), and strains were 0.17 and 0.28 %, respectively. The displacement of NPI-30 actuator was 1.1 mm and the strain was 0.06 %, which were lowest among the actuators due to the stiffness of the actuator. At 1.0 Hz, as shown in Figure 3.9 (c), the displacement of Nafion 117 and NPI-18 actuators were 1.3 and 2.0 mm, and strains were 0.07 and 0.14 %, respectively. The displacement of NPI-30 actuator was 1.1 mm and the strain was 0.06 %, which were lowest.

The displacement decreases at 1.0 Hz compared to 0.5 Hz and the displacement responses are slower compared to 0.5 Hz. These effects are thought to be due to the limited charging time at higher frequency [46]. As the actuating frequency increases, the charging time for the hydrated cations to move toward the anode becomes shorter, resulting in the decrease of both displacement and strain. From the displacement results, we could see comparable electromechanical performance even with significant amount of 18 wt.% of PI in the actuator.

The photographic images of prepared IPMC actuators at maximum displacement with/without applying voltage (± 3 V, AC) under varied frequency (0.1, 0.5, and 1.0 Hz) are shown in Figure 3.10. It shows that the NPI-18 IPMC actuator demonstrated the similar displacement range compared to Nafion 117 IPMC actuator. NPI-30 IPMC actuator showed lowest degree of deformation among the actuators. The photographic images correspond with the displacement performances.



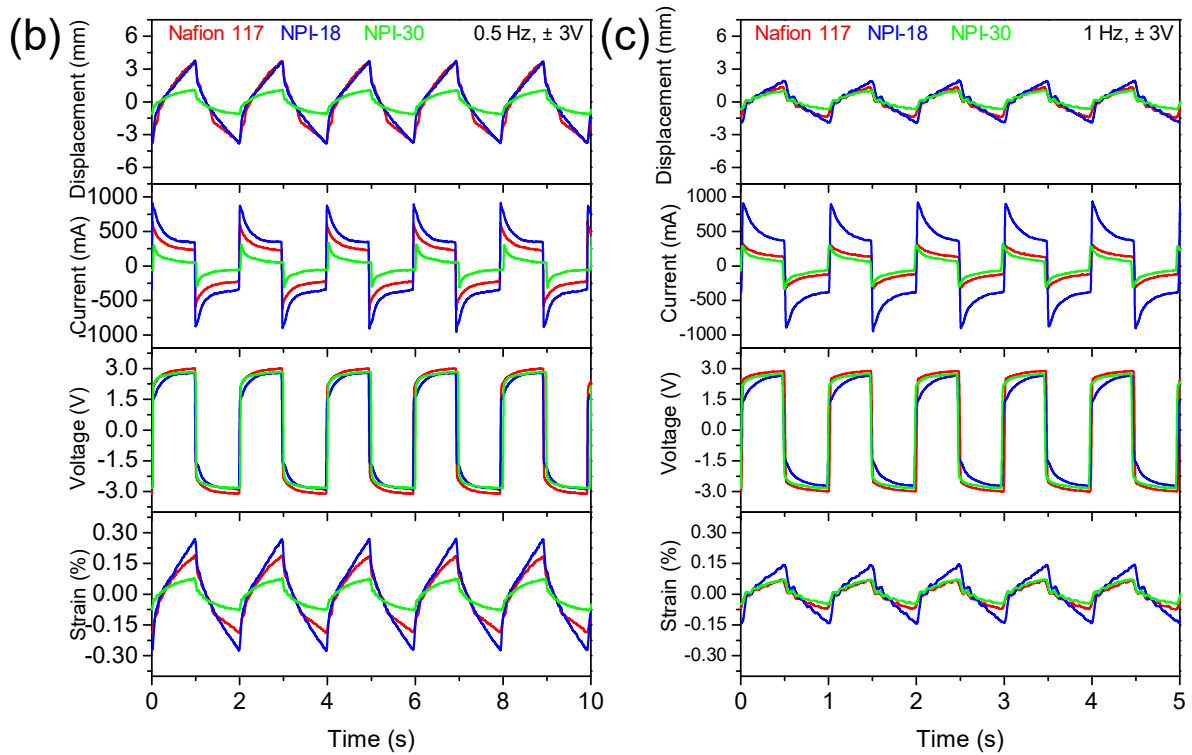


Figure 3.9 The actuation performance of the IPMC actuators (Nafion 117, NPI-18, and NPI-30) : measured voltage, current, displacement responses, and bending strain at ± 3 V, AC square-wave under (a) 0.1 Hz, (b) 0.5 Hz, and (c) 1.0 Hz. Superimposed image of video captures of NPI-18 actuator at 0.1 Hz is also included in (a) clearly exhibiting the bounce-back effect of PI-incorporated actuator system.

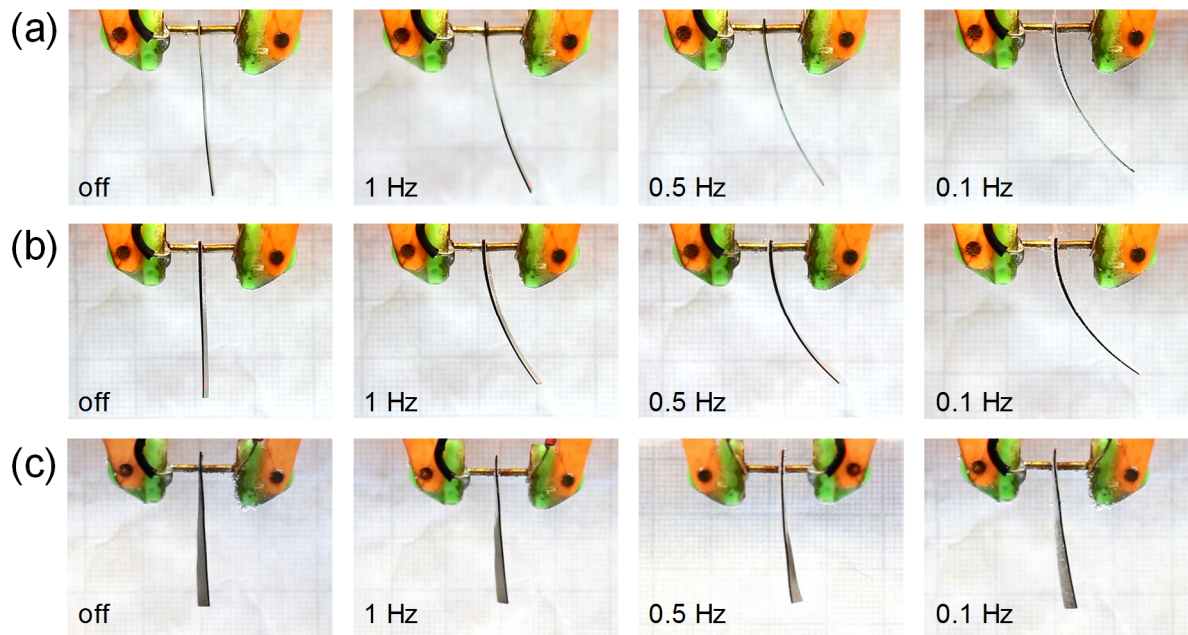


Figure 3.10 Photographic images of prepared IPMC actuators, (a) Nafion 117, (b) NPI-18, and (c) NPI-30 with/without applying voltage (± 3 V, AC) under varied frequency (0.1, 0.5, and 1.0 Hz).

3.6.3 Blocking forces of IPMCs

The blocking force, which represents the electromechanical force formed at the tip of IPMC at zero displacement, was measured under driving voltage of 3V, DC. Figure 3.11 shows the typical blocking force responses measured in time for Nafion 117 and NPI-18 actuators. The highest blocking forces of Nafion 117 and NPI-18 were measured to 6.86 mN at 1.84 s and 5.93 mN at 1.47 s. The blocking for decrease of NPI-18 is likely to come from the increased stiffness of PI incorporated in Nafion. The blocking force is decreased by less than 15 % and the response time is also decreased by 20 %. While obtaining faster response time of actuators

by blending PI is important, the decrease in blocking force that accompanies should also be considered in the fabrication of IPMC actuators. We believe that NPI-18 could give better actuation performance by providing faster response time that is usually needed in IPMC actuators.

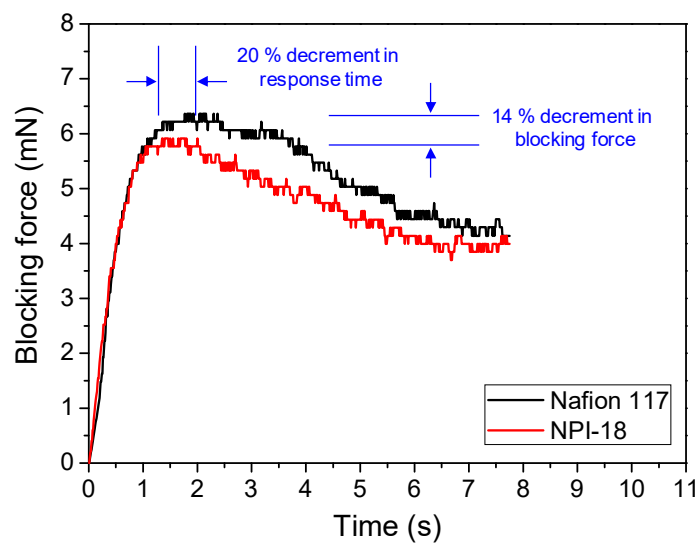


Figure 3.11 Blocking force responses in time at 3 V, DC for IPMC actuators comparing Nafion 117 and NPI-18.

3.7 Conclusions

We successfully casted blend membranes of Nafion and PI using a precursor polymer method, which are used as ion exchange membranes that could be fabricated into

IPMCs. The Nafion/PAA blend membranes were successfully successfully via solution casting method, which underwent thermal imidization to form Nafion/PI. To our knowledge, it is the first example to prepare Nafion/PI membrane. The blend membranes were characterized by FT-IR, TGA, and DMA. FT-IR results confirmed the success of thermal imidization process and the presence of both components, Nafion and PI in the blend membranes. Thermal properties were characterized using TGA, which confirmed the presence of both components in the blends. DMA results showed that as the content of PI increases, elasticity of the material increases while damping of the material decreases. The mechanical properties characterized by DMA, suggests the possibility of controlling elasticity and the degree of damping of materials by varying the content of PI in the blends. The blend membranes were fabricated into IPMCs using the conventional platinum electroless plating process of Nafion. Fabricated IPMCs were characterized by SEM and the actuation performance were investigated. Through surface resistance and SEM results, solution casted Nafion, NPI-6, and NPI-12 IPMCs were not qualified to do actuation testing. We chose Nafion 117, NPI-18, and NPI-30 IPMCs to compare the actuation performance. As a result, Nafion-PI blend actuator showed comparable actuation performance including displacement and blocking forces compared to commercially available Nafion 117 even though we reduced the content of Nafion by 18 wt.% (weight percent ratio of Nafion:PI = 82:18) while improving both thermal and mechanical properties.

3.8 Future studies

Future studies will be dedicated to investigating other types of polymers to blend with Nafion that can improve or control chemical and mechanical properties ion exchange

membranes while maintaining electromechanical performances. As one of the attempts, we could expand Nafion-PI project by developing different types of PIs as blending partners. By synthesizing different types of PIs using different types of dianhydrides and dianilines, we may be able to modify properties of PIs such as solubility, dimensional stability, and thermal properties, etc. Using different types of PIs to blend with Nafion to make new types of IPMCs, we can expect to modify various properties of Nafion.

REFERENCES

1. Terasawa, N., et al., *High-performance polymer actuators based on poly(ethylene oxide) and single-walled carbon nanotube–ionic liquid-based gels*. Sensors and Actuators B: Chemical, 2014. **202**: p. 382-387.
2. Liu, Z. and P. Calvert, *Multilayer Hydrogels as Muscle-Like Actuators*. Advanced Materials, 2000. **12**(4): p. 288-291.
3. Shiga, T., et al., *Bending of ionic polymer gel caused by swelling under sinusoidally varying electric fields*. Journal of Applied Polymer Science, 1993. **47**(1): p. 113-119.
4. Shahinpoor, M., *Conceptual design, kinematics and dynamics of swimming robotic structures using ionic polymeric gel muscles*. Smart Materials and Structures, 1992. **1**(1): p. 91.
5. Jung, K., K.J. Kim, and H.R. Choi, *A self-sensing dielectric elastomer actuator*. Sensors and Actuators A: Physical, 2008. **143**(2): p. 343-351.
6. Pelrine, R., et al., *High-Speed Electrically Actuated Elastomers with Strain Greater Than 100%*. Science, 2000. **287**(5454): p. 836-839.
7. Jeon, T.-I., et al., *Optical and electrical properties of preferentially anisotropic single-walled carbon-nanotube films in terahertz region*. Journal of Applied Physics, 2004. **95**(10): p. 5736-5740.
8. Kim, J.H., et al., *Fabrication and electrochemical properties of carbon nanotube film electrodes*. Carbon, 2006. **44**(10): p. 1963-1968.
9. Mohsen, S. and J.K. Kwang, *Ionic polymer-metal composites: I. Fundamentals*. Smart Materials and Structures, 2001. **10**(4): p. 819.

10. Sangki, L., P. Hoon Cheol, and K. Kwang Jin, *Equivalent modeling for ionic polymer–metal composite actuators based on beam theories*. Smart Materials and Structures, 2005. **14**(6): p. 1363.
11. Sang-Mun, K. and J.K. Kwang, *Palladium buffer-layered high performance ionic polymer–metal composites*. Smart Materials and Structures, 2008. **17**(3): p. 035011.
12. Kim, D., et al., *Electro-chemical operation of ionic polymer–metal composites*. Sensors and Actuators B: Chemical, 2011. **155**(1): p. 106-113.
13. Kim, S.J., et al., *A bio-inspired multi degree of freedom actuator based on a novel cylindrical ionic polymer–metal composite material*. Robotics and Autonomous Systems, 2014. **62**(1): p. 53-60.
14. Shen, Q., et al., *A biomimetic underwater vehicle actuated by waves with ionic polymer–metal composite soft sensors*. Bioinspiration & Biomimetics, 2015. **10**(5): p. 055007.
15. Palmre, V., et al., *An IPMC-enabled bio-inspired bending/twisting fin for underwater applications*. Smart Materials and Structures, 2013. **22**(1): p. 014003.
16. Lee, S. and Kim, K.J., *Design of IPMC actuator-driven valve-less micropump and its flow rate estimation at low Reynolds numbers*. Smart Materials and Structures, 2006. **15**(4): p. 1103.
17. Lu, J., et al., *A Biomimetic Actuator Based on an Ionic Networking Membrane of Poly(styrene-alt-maleimide)-Incorporated Poly(vinylidene fluoride)*. Advanced Functional Materials, 2008. **18**(8): p. 1290-1298.
18. Mohsen, S. and J.K. Kwang, *Ionic polymer–metal composites: IV. Industrial and medical applications*. Smart Materials and Structures, 2005. **14**(1): p. 197.
19. Jung, K., J. Nam, and H. Choi, *Investigations on actuation characteristics of IPMC artificial muscle actuator*. Sensors and Actuators A: Physical, 2003. **107**(2): p. 183-192.

20. Katchalsky, A., *Rapid swelling and deswelling of reversible gels of polymeric acids by ionization*. *Experientia*, 1949. **5**(8): p. 319-320.
21. Kuhn, W., *Valenter Fadenmolekülionen*. *Exper*, 1949. **5**: p. 318.
22. Kuhn, W., et al., *Reversible Dilation and Contraction by Changing the State of Ionization of High-Polymer Acid Networks*. *Nature*, 1950. **165**(4196): p. 514-516.
23. Li, Y. and T. Tanaka, *Kinetics of swelling and shrinking of gels*. *The Journal of Chemical Physics*, 1990. **92**(2): p. 1365-1371.
24. De Rossi, D.E., et al., *Contractile behavior of electrically activated mechanochemical polymer actuators*. *ASAIO transactions / American Society for Artificial Internal Organs*, 1986. **32**(1): p. 157-162.
25. Caldwell, D.G. and P.M. Taylor, *Chemically stimulated pseudo-muscular actuation*. *International Journal of Engineering Science*, 1990. **28**(8): p. 797-808.
26. Hamlen, R.P., C.E. Kent, and S.N. Shafer, *Electrolytically Activated Contractile Polymer*. *Nature*, 1965. **206**(4989): p. 1149-1150.
27. Oguro, K., Y. Kawami, and H. Takenaka, *Bending of an ion-conducting polymer film-electrode composite by an electric stimulus at low voltage*. *Journal of Micromachine Society*, 1992. **5**(1): p. 27-30.
28. Kwan, D.N.C.N.a.A.K., *Ionic Polymer Metal Composite Transducer and Self-Sensing Ability, Smart Actuation and Sensing Systems*. 2012.
29. Jin, W., et al., *A Flemion-based actuator with ionic liquid as solvent*. *Smart Materials and Structures*, 2007. **16**(2): p. S214.
30. Wang, J., et al., *Bioinspired design of tactile sensors based on Flemion*. *Journal of Applied Physics*, 2009. **105**(8): p. 083515.
31. Kim, K.J. and M. Shahinpoor, *A novel method of manufacturing three-dimensional ionic*

- polymer–metal composites (IPMCs) biomimetic sensors, actuators and artificial muscles.* Polymer, 2002. **43**(3): p. 797-802.
32. Lee, J.H., et al., *Water uptake and migration effects of electroactive ion-exchange polymer metal composite (IPMC) actuator.* Sensors and Actuators A: Physical, 2005. **118**(1): p. 98-106.
 33. Jung, W., S.-S. Kang, and Y. Toi, *Computational modeling of electrochemical–mechanical behaviors of Flemion-based actuators considering the effects of electro-osmosis and electrolysis.* Computers & Structures, 2010. **88**(15–16): p. 938-948.
 34. Yoon, W.J., P.G. Reinhall, and E.J. Seibel, *Analysis of electro-active polymer bending: A component in a low cost ultrathin scanning endoscope.* Sensors and Actuators A: Physical, 2007. **133**(2): p. 506-517.
 35. Nemat-Nasser, S. and Y. Wu, *Comparative experimental study of ionic polymer–metal composites with different backbone ionomers and in various cation forms.* Journal of Applied Physics, 2003. **93**(9): p. 5255-5267.
 36. Fujiwara, N., et al., *Preparation of Gold–Solid Polymer Electrolyte Composites As Electric Stimuli-Responsive Materials.* Chemistry of Materials, 2000. **12**(6): p. 1750-1754.
 37. Tiwari, R. and E. Garcia, *The state of understanding of ionic polymer metal composite architecture: a review.* Smart Materials and Structures, 2011. **20**(8): p. 083001.
 38. Fukushima, K., et al., *Ion-dissociative functional compound, method for production thereof, ionic conductor, and electrochemical device.* 2011, Google Patents.
 39. Panwar, V., et al., *New ionic polymer–metal composite actuators based on PVDF/PSSA/PVP polymer blend membrane.* Polymer Engineering & Science, 2011. **51**(9): p. 1730-1741.
 40. Han, M.J., et al., *Ionic Polymer-Metal Composite Actuators Employing Radiation-Grafted*

- Fluoropolymers as Ion-Exchange Membranes*. Macromolecular Rapid Communications, 2006. **27**(3): p. 219-222.
41. Jeon, J.-H., et al., *Novel biomimetic actuator based on SPEEK and PVDF*. Sensors and Actuators B: Chemical, 2009. **143**(1): p. 357-364.
 42. Phillips, A.K. and R.B. Moore, *Ionic actuators based on novel sulfonated ethylene vinyl alcohol copolymer membranes*. Polymer, 2005. **46**(18): p. 7788-7802.
 43. Lagaron, J.M., R. Catalá, and R. Gavara, *Structural characteristics defining high barrier properties in polymeric materials*. Materials Science and Technology, 2004. **20**(1): p. 1-7.
 44. Li, M., et al., *High performance filtration nanofibrous membranes based on hydrophilic poly(vinyl alcohol-co-ethylene) copolymer*. Desalination, 2013. **329**: p. 50-56.
 45. Jo, C., et al., *Recent advances in ionic polymer-metal composite actuators and their modeling and applications*. Progress in Polymer Science, 2013. **38**(7): p. 1037-1066.
 46. Palmre, V., et al., *Nanoothorn electrodes for ionic polymer-metal composite artificial muscles*. Scientific Reports, 2014. **4**: p. 6176.
 47. Hwang, T., et al., *A new ionic polymer-metal composite based on Nafion/poly(vinyl alcohol-co-ethylene) blends*. Smart Materials and Structures, 2015. **24**(10): p. 105011.
 48. Duncan, A.J., D.J. Leo, and T.E. Long, *Beyond Nafion: Charged Macromolecules Tailored for Performance as Ionic Polymer Transducers*. Macromolecules, 2008. **41**(21): p. 7765-7775.
 49. Jeong, H.M., et al., *Preparation and characterization of electroactive acrylic polymer-platinum composites*. Macromolecular Research. **12**(6): p. 593-597.
 50. Wang, X.-L., et al., *Biomimetic electro-active polymer based on sulfonated poly (styrene-b-ethylene-co-butylene-b-styrene)*. Materials Letters, 2007. **61**(29): p. 5117-5120.
 51. Wang, X.-L., I.-K. Oh, and J.-B. Kim, *Enhanced electromechanical performance of*

- carbon nano-fiber reinforced sulfonated poly(styrene-*b*-[ethylene/butylene]-*b*-styrene) actuator*. Composites Science and Technology, 2009. **69**(13): p. 2098-2101.
52. Silva, R.F., S. Passerini, and A. Pozio, *Solution-cast Nafion®/montmorillonite composite membrane with low methanol permeability*. Electrochimica Acta, 2005. **50**(13): p. 2639-2645.
53. Liu, J., et al., *Nafion–polyfurfuryl alcohol nanocomposite membranes for direct methanol fuel cells*. Journal of Membrane Science, 2005. **246**(1): p. 95-101.
54. Aricò, A.S., et al., *Influence of the acid–base characteristics of inorganic fillers on the high temperature performance of composite membranes in direct methanol fuel cells*. Solid State Ionics, 2003. **161**(3–4): p. 251-265.
55. Lebrun, L., E. Da Silva, and M. Metayer, *Elaboration of ion-exchange membranes with semi-interpenetrating polymer networks containing poly(vinyl alcohol) as polymer matrix*. Journal of Applied Polymer Science, 2002. **84**(8): p. 1572-1580.
56. IWASEYA, M., et al., *High performance films obtained from PVA/Na₂SO₄/H₂O and PVA/CH₃COONa/H₂O systems*. Journal of Materials Science, 2005. **40**(21): p. 5695-5698.
57. Li, G.H., et al., *Preparation of poly(vinyl phosphate-*b*-styrene) copolymers and its blend with PPO as proton exchange membrane for DMFC applications*. Solid State Ionics, 2006. **177**(11–12): p. 1083-1090.
58. Gruger, A., et al., *Nanostructure of Nafion® membranes at different states of hydration: An IR and Raman study*. Vibrational Spectroscopy, 2001. **26**(2): p. 215-225.
59. Wang, C., et al., *Preparation of amino-functionalized graphene oxide/polyimide composite films with improved mechanical, thermal and hydrophobic properties*. Applied Surface Science, 2016. **362**: p. 11-19.
60. Varganici, C.-D., et al., *On the thermal stability of some aromatic-aliphatic polyimides*.

- Journal of Analytical and Applied Pyrolysis, 2015. **113**: p. 390-401.
61. Song, G., et al., *Negative in-plane CTE of benzimidazole-based polyimide film and its thermal expansion behavior*. Polymer, 2014. **55**(15): p. 3242-3246.
 62. Asano, N., et al., *Aliphatic/Aromatic Polyimide Ionomers as a Proton Conductive Membrane for Fuel Cell Applications*. Journal of the American Chemical Society, 2006. **128**(5): p. 1762-1769.
 63. Lee, S.-Y., et al., *Nonhumidified Intermediate Temperature Fuel Cells Using Protic Ionic Liquids*. Journal of the American Chemical Society, 2010. **132**(28): p. 9764-9773.
 64. Einsla, B.R., et al., *Sulfonated naphthalene dianhydride based polyimide copolymers for proton-exchange-membrane fuel cells. I. Monomer and copolymer synthesis*. Journal of Polymer Science Part A: Polymer Chemistry, 2004. **42**(4): p. 862-874.
 65. Einsla, B.R., et al., *Sulfonated naphthalene dianhydride based polyimide copolymers for proton-exchange-membrane fuel cells: II. Membrane properties and fuel cell performance*. Journal of Membrane Science, 2005. **255**(1-2): p. 141-148.
 66. Fang, J., et al., *Novel Sulfonated Polyimides as Polyelectrolytes for Fuel Cell Application. I. Synthesis, Proton Conductivity, and Water Stability of Polyimides from 4,4'-Diaminodiphenyl Ether-2,2'-disulfonic Acid*. Macromolecules, 2002. **35**(24): p. 9022-9028.
 67. Woo, Y., et al., *Synthesis and characterization of sulfonated polyimide membranes for direct methanol fuel cell*. Journal of Membrane Science, 2003. **220**(1-2): p. 31-45.
 68. Song, J., et al., *Electro-active Polymer Actuator Based on Sulfonated Polyimide with Highly Conductive Silver Electrodes Via Self-metallization*. Macromolecular Rapid Communications, 2011. **32**(19): p. 1583-1587.
 69. Imaizumi, S., et al., *Printable Polymer Actuators from Ionic Liquid, Soluble Polyimide,*

- and Ubiquitous Carbon Materials*. ACS Applied Materials & Interfaces, 2013. **5**(13): p. 6307-6315.
70. Kumar, A., et al., *¹H NMR and FT-IR dataset based structural investigation of poly(amic acid)s and polyimides from 4,4'-diaminostilbene*. Data in Brief, 2016. **7**: p. 123-128.
71. Laporta, M., M. Pegoraro, and L. Zanderighi, *Perfluorosulfonated membrane (Nafion): FT-IR study of the state of water with increasing humidity*. Physical Chemistry Chemical Physics, 1999. **1**(19): p. 4619-4628.
72. Chen, Q., et al., *Identification of the testing parameters in high frequency dynamic shear measurement on agarose gels*. Journal of Biomechanics, 2005. **38**(4): p. 959-963.
73. Bashaiwoldu, A.B., F. Podczeck, and J.M. Newton, *Application of dynamic mechanical analysis (DMA) to determine the mechanical properties of pellets*. International Journal of Pharmaceutics, 2004. **269**(2): p. 329-342.
74. Zhimin, X., et al., *Dynamic Mechanical Properties of Aged Filled Rubbers*. Journal of Macromolecular Science: Physics, 2004. **43**(4): p. 805-817.

CURRICULUM VITAE

Graduate College
University of Nevada, Las Vegas

Jungsoo Nam

Degrees:

Bachelor of Science in Chemistry & Nano Science, 2014

Ewha Womans University

Seoul, 03760

Publications:

1. Soo-Yeon Moon, **Jungsoo Nam**, Kris Rathwell, and Won-Suk Kim; “Copper-Catalyzed Chan–Lam Coupling between Sulfonyl Azides and Boronic Acids at Room Temperature” *Organic Letters*, **2014**, 16, 338-341.
2. Taeseon Hwang, Viljar Palmre, **Jungsoo Nam**, Dong-Chan Lee, and Kwang J Kim; “A new ionic polymer–metal composite based on Nafion/poly(vinyl alcohol-co-ethylene) blends” *Smart Mater. Struct.* **2015**, 24, 105011.

Thesis Title:

Ionic Polymer-Metal Composite Actuators based on Nafion Blends with Functional Polymers

Thesis Examination Committee:

Chairperson, Dong-Chan Lee, Ph.D.

Committee Member, Kathleen A. Robins, Ph.D.

Committee Member, Gary Kleiger, Ph.D.

Graduate Faculty Representative, Kwang J. Kim, Ph.D.